Spectral Factor Model for Corporate Bonds: Separating Signal from Noise

Twan R. Mulder[*]   Maria Grith [†]   Patrick Verwijmeren [§]

Abstract

This paper introduces the analysis of factor models in the frequency domain to the corporate bond pricing literature, using the *spectral factor model* developed by Bandi, Chaudhuri, Lo and Tamoni (2021). We decompose the bond market factor into orthogonal frequency-specific components, where the *spectral betas* capture frequency-specific systematic risk. Our findings show that an *annual cycle* component of the bond market factor—spanning 8 to 16 months—enhances the bond CAPM. In earlier literature, a liquidity risk factor adds incremental cross-sectional pricing power beyond the bond market factor. We show that when the bond market factor is substituted by its annual cycle component, the liquidity risk factor loses its incremental pricing power. Supported by additional evidence, we conclude that the annual cycle component can be interpreted as the *liquidity cycle* of the bond market factor. Moreover, the results indicate that dimensionality reduction in factor models can be achieved by separating *signal* from *noise* in the frequency domain.

Keywords: Corporate bonds, Cross-sectional asset pricing, Factor models, Frequency, Systematic risk

JEL classification: C12, C13, E32, G12

---

[*]Email: twan.mulder@gtc.ox.ac.uk. Department of Statistics, Oxford University, UK

[†]Email: grith@ese.eur.nl. Erasmus School of Economics, Erasmus University Rotterdam, The Netherlands

[‡]Email: verwijmeren@ese.eur.nl. Erasmus School of Economics, Erasmus University Rotterdam, The Netherlands

1 Introduction

In 2022, the market value of global fixed income outstanding reached 129.8 trillion USD, while the global equity market capitalisation was 101.2 trillion USD (SIFMA, 2023). Firms issued 1.4 trillion USD in corporate bonds in 2022, whereas equity issuances amounted to 99.4 billion USD. Despite the vast size of the corporate bond market, the literature on asset pricing has traditionally paid more attention to equities than corporate bonds (Kelly, Palhares & Pruitt, 2023). Recently, however, there has been a growing interest in identifying corporate bond risk factors.[*] We contribute to this literature by introducing analysis in the frequency domain to corporate bond pricing. Specifically, we examine whether, and if so which, frequency-specific risk factors can explain the cross-sectional variation in expected returns on corporate bond portfolios.

Using factor models, systematic risk—or beta, in finance jargon—is usually estimated with monthly (excess) asset returns. For example, in the capital asset pricing model (CAPM) of Sharpe (1964) and Lintner (1975), the beta of an asset is estimated by regressing its monthly excess returns on the excess market returns. However, aside from the assumption that investors maximise *single-period* utility, the CAPM does not impose restrictions that prevent its estimation using yearly, quarterly, or daily returns (Bandi & Tamoni, 2022). It is well documented, though, that the estimated betas differ across these estimation horizons (e.g., Levhari & Levy, 1977). While previous literature attributed these horizon-specific betas to statistical biases, such as serial cross-correlation in returns caused by trading frictions (Scholes & Williams, 1977), more recent literature views it as capturing frequency-specific risk, and thus an economic phenomenon (Bandi & Tamoni, 2022). Specifically, investors with different investment horizons may encounter varying levels of systematic risk. This variation can be explained by the delayed adjustment of asset returns to new information about risk factors (Kamara, Korajczyk, Lou & Sadka, 2016). Therefore, especially in the over-the-counter corporate bond market, where illiquidity and high trading costs lead to infrequent trading, systematic risk is likely to be frequency-dependent, and horizon-specific asset pricing effects are expected to be observed.

While traditional factor models, such as the CAPM, do not impose restrictions on the horizon over which returns should be measured, recent literature has shown that these models implicitly restrict systematic risk to be constant across frequencies (Bandi et al., 2021). Therefore, in this paper, we use the *spectral factor model* introduced by Bandi et al. (2021), which is designed to capture frequency-dependent systematic risk explicitly. This approach may lead to economically motivated dimensionality reduction in factor models. For example, from an economic perspective, it makes sense that the CAPM betas price the cross-section of expected equity returns (Bandi & Tamoni, 2022). However, literature has shown that the CAPM does not perform well in empirical applications. Bandi et al. (2021) find that a spectral CAPM—which includes only a business cycle component of the stock market factor—can explain the cross-section of expected equity returns.

In this paper, we investigate whether the spectral factor model, as introduced by Bandi et

---

[*]See, for instance, Bai, Bali and Wen (2019); Kelly et al. (2023); Dickerson, Mueller and Robotti (2023); Dickerson, Julliard and Mueller (2023); Dick-Nielsen, Feldhütter, Pedersen and Stolborg (2023); van Binsbergen, Nozawa and Schwert (2023); Elkamhi, Jo and Nozawa (2024) and Dickerson and Nozawa (2024)

al. (2021), can be used to achieve dimensionality reduction in the corporate bond factor space. Specifically, we decompose the bond market factor (MKTB) into frequency-specific components, which are then used in a linear factor model. The resulting *spectral* bond CAPM (CAPMB) is evaluated against traded- and nontraded-factor models proposed in the recent corporate bond pricing literature. Furthermore, we identify the frequency-specific component of MKTB that contains the strongest pricing signal and examine its potential to crowd out other risk factors in multifactor models. This investigation is relevant for several reasons. First, previous findings suggest that the CAPMB is a strong factor model, outperforming other (multi)factor models (Dickerson, Mueller & Robotti, 2023). Therefore, the decomposition of MKTB into frequency-specific components may provide valuable insights into the cross-sectional determinants of corporate bond returns.[†] Moreover, recent literature shows that only a liquidity-risk factor adds incremental cross-sectional pricing power beyond MKTB (Dickerson, Mueller & Robotti, 2023). Therefore, it is interesting to investigate whether a frequency-specific component of MKTB can crowd out liquidity risk.

The spectral factor model is based on the observation that any covariance-stationary time series—to which, thus, the Wold (1938) representation applies—can be decomposed in an infinite sum of orthogonal frequency-specific components (Ortu, Severino, Tamoni & Tebaldi, 2020). Using this *extended Wold* decomposition on risk factors, we obtain orthogonal components that capture fluctuations of the original risk factors and which are associated with a specific periodicity. These frequency-specific components of the risk factor are termed *spectral factors*. When the spectral factors are used in a linear factor model, we obtain *spectral betas* that capture systematic risk associated with cycles of different lengths. Moreover, it can be shown that the beta of a traditional factor model is a weighted average of the spectral betas (Bandi et al., 2021). Therefore, traditional factor models assume that the spectral betas are constant across frequencies, and thus also systematic risk. In the spectral factor model, however, systematic risk is allowed to vary with frequency. Besides that, unlike other common methods in macro-finance for extracting frequency-specific components, such as multiresolution (wavelet) filters, the extended Wold decomposition is particularly suitable for our asset-pricing context. Specifically, because of the orthogonality of the spectral factors, the spectral betas can immediately be used in the second pass regression to determine the incremental cross-sectional explanatory power of the spectral factors (Cochrane, 2009; Kan, Robotti & Shanken, 2013). This is because the multiple regression betas are equivalent to the simple regression betas.

Additionally, we employ identification- and misspecification-robust regression techniques. This is important in the context of corporate bond pricing since recent studies have addressed a credibility and replication crisis, attributed to unreliable data sources and the absence of a standardised framework for evaluating factor models (Dick-Nielsen et al., 2023; Dickerson, Mueller & Robotti, 2023). Therefore, we adopt the model-misspecification-robust standard errors proposed by Kan et al. (2013) and present the prices of covariance risk estimated using both ordinary least squares (OLS) and generalised least squares (GLS) regression techniques,

---

[†]This reason is explicitly mentioned by Dickerson, Mueller and Robotti (2023) to motivate the decomposition of corporate bond risk factors into frequency-specific components as an interesting area for future research. This underscores the significance of our work from an academic perspective. Since, up to our knowledge, we are the first to analyse corporate bond pricing in the frequency domain.

following Lewellen, Nagel and Shanken (2010).

We collect intraday transaction data for corporate bonds from the Trade Reporting and Compliance Engine (TRACE) database. Following the framework outlined by Dickerson, Mueller and Robotti (2023), this data is further cleaned with bond characteristic data collected from the Fixed Income Securities Database (FISD). Ultimately, the intraday returns are aggregated to a monthly time series. Moreover, the factor models are evaluated on a diverse set of test portfolios. We consider a set of 32 portfolios that are constructed by sorting bonds on industry classification, credit spread and rating.

Our main finding is that an *annual cycle* component of the bond market factor—capturing fluctuations between 8 and 16 months—contains the most signal for explaining the cross-section of expected corporate bond returns. The resulting *spectral CAPMB*, containing this annual cycle component of the bond market factor, obtains a higher cross-sectional $\mathbb{R}^2$ than the bond CAPM itself. Furthermore, we also compare the spectral CAPMB with other popular (multi)factor models, such as the intermediary asset pricing model of He, Kelly and Manela (2017), following the framework proposed by Dickerson, Mueller and Robotti (2023).

Moreover, we show that the spectral factors lead to dimensionality reduction in corporate bond factor models. For instance, in the four-factor model of Bai et al. (2019)—consisting of the bond market factor and a default, liquidity and credit risk factor—we show that only the liquidity risk factor has incremental cross-sectional pricing power, which has previously been documented by Dickerson, Mueller and Robotti (2023). Interestingly, when the bond market factor is substituted by its annual cycle component, the liquidity risk factor in this four-factor model loses its incremental explanatory power. This finding indicates that the annual cycle component captures (at least some of) the information contained in the liquidity risk factor. Therefore, this annual cycle component can be interpreted as the *liquidity cycle* of the bond market factor. Furthermore, consistent with previous literature, we show that liquidity risk is priced over the short term (Kamara et al., 2016).

The remainder of this paper is structured as follows. In Section 2, we discuss related literature. In Section 3, we introduce the spectral factor model of Bandi et al. (2021) and discuss the identification of the spectral components. Then, in Section 4, we describe the data. In Section 5 we present the results and evaluate the performance of the spectral factor model in pricing the cross-section of expected corporate bond returns. Finally, we conclude this paper in Section 6.

2   Literature review

This paper contributes to the literature that uses spectral analysis to study economic processes in the frequency domain. A prominent example is the work of Nobel laureate Friedman (1957), who, by decomposing income into a transitory and permanent component, concludes that consumption is influenced by permanent income shocks rather than by changes in transitory income. Similarly, Engle (1978) finds that output prices are more elastic with respect to wages at lower frequencies compared to higher frequencies. These studies, among many others in macroeconomics, use spectrum regression to analyse the dependence of economic variables in the frequency

domain.‡ In *spectrum regressions*, the dependent and independent variables are first Fourier-transformed before being used in regression models (Hannan, 1963b, 1963a; Bandi & Tamoni, 2022).

While the literature mentioned above is mainly concerned with frequency-specific relationships in the macro-economy, the finance literature has also applied spectrum regressions. For instance, Chaudhuri and Lo (2018) use the Fourier-transform to separate and evaluate the static and dynamic components of an investment portfolio's performance, where the resulting dynamic alpha measures the portfolio manager's ability across different time horizons. Additionally, Chaudhuri and Lo (2015) use spectral analysis to study the volatility and correlation between individual stock returns across different frequencies.

Instead, this paper contributes to the finance literature that documents the variation in betas and risk premia across frequencies. A common approach to estimating the capital asset pricing model (CAPM) is by using monthly excess asset returns and monthly excess market returns. However, the CAPM, as introduced by Sharpe (1964) and Lintner (1975), does not specify the time horizon for estimation. Rather it only assumes that investors maximise *single-period* utility (Levhari & Levy, 1977; Bandi & Tamoni, 2022). Therefore, market betas can be estimated using returns measured over any reasonable horizon, whether daily, weekly or monthly. Nevertheless, literature has shown that the estimates of systematic risk (i.e., betas) and the corresponding risk premia differ across these horizons. This literature can be categorised into four streams, which are discussed next (Bandi et al., 2021).

The first stream of literature employs spectral analysis, as discussed above. For example, Goldberg and Vora (1978) use spectral analysis to study the frequency-specific relationship between returns on public utility firms and the market. They conclude that the CAPM betas vary across cycles of different durations. Dew-Becker and Giglio (2016) use a frequency-based decomposition of the stochastic discount factor (SDF) to extract frequency-specific prices of risk, demonstrating that long-run risk cycles are priced significantly in the economy. Furthermore, Neuhierl and Varneskov (2021) developed a model-free framework to decompose the SDF into permanent and transitory components, revealing the presence of both low- and high-frequency priced risk factors.

However, a more common approach to study frequency-specific betas has been *aggregation*—the accumulation of excess asset returns and risk factors over a specific horizon (Bandi & Tamoni, 2022). For example, Levhari and Levy (1977) show that the betas of the stock market factor in the CAPM are affected by the investment horizon (i.e., the horizon over which returns are measured). Moreover, Hawawini (1983) finds that the market betas of small firms decrease as the investment horizon shortens, whereas those of big firms increase. This is a problem, since it may falsely indicate that small firms are less riskier when shorter return intervals are used for estimation. Additionally, Schwartz and Whitcomb (1977) document a decline in the cross-sectional R^2 of the CAPM when shorter intervals are used to calculate returns.

The third stream of literature shows that the betas are sensitive to the rebalancing frequency of the test portfolios (Handa, Kothari & Wasley, 1989; Kothari, Shanken & Sloan, 1995). For instance, Cohen, Polk and Vuolteenaho (2009) find that the CAPM betas of low book-to-market

---

‡See Bandi and Tamoni (2022, Section 2.1) for an extensive review.

(growth) portfolios are higher immediately after the sort, compared to the betas of high book-to-market (value) portfolios. However, over the long run—such as 10 to 15 years after the sorting—the CAPM betas of growth portfolios are lower than those of value portfolios.

The fourth stream uses multiresolution analysis—specifically, wavelet filters—to study the dependence of betas over frequencies. For example, Gençay, Selçuk and Whitcher (2003) decompose the market factor and excess asset returns using wavelet filters to derive frequency-specific betas. They conclude that the CAPM performs more accurately over the medium- to long-run. Similarly, Kang, In and Kim (2017) use wavelet filters to obtain betas in the time-scale domain, and conclude that a business-cycle component of the Fama and French (1993) three-factor model enhances the cross-sectional pricing accuracy of the model itself. Furthermore, Ortu, Tamoni and Tebaldi (2013) use the Haar filter to decompose consumption growth into frequency-specific components, and conclude that a low-frequency component commands a 2% premium per annum.

In this paper, the frequency decomposition is related to this last approach, multiresolution analysis. We use the *extended Wold representation* introduced by Bandi, Perron, Tamoni and Tebaldi (2019) and Ortu et al. (2020). This approach applies the Haar filter to the shocks of the Wold (1938) representation rather than the process itself. Therefore, while multiresolution filters are non-parametric, the extended Wold representation defines a *data generating process*, which is parametric and thus needs to be identified. Since the extended Wold representation provides an explicit relationship between a model in the time domain and a model in the time-scale domain, it has two advantages over multiresolution analysis (Bandi & Tamoni, 2022). First, it enhances economic interpretability. For instance, in Appendix D, we derive the relationship between spectral betas in the time-scale domain and delayed price adjustment to risk factors in the time domain. Second, it facilitates the use of more robust inferential techniques, which are often developed for time series (i.e., in the time domain).

Bandi et al. (2021) also use the extended Wold representation to introduce the *spectral factor model*, where the excess asset returns and risk factors are decomposed into frequency-specific components. The resulting factor loadings are called *spectral betas*. Bandi et al. (2021) show that the aggregate beta in the traditional factor model is a weighted average of the spectral betas. This implies that the traditional factor model assumes equal spectral betas across frequencies, and is, therefore, unable to capture frequency-specific risk. Moreover, Bandi et al. (2021) find that the *spectral CAPM*—consisting of only the frequency-specific component of the excess market return that captures cycles between 32 and 64 months (i.e., the business cycle component)—improves the cross-sectional pricing accuracy of the CAPM substantially. This paper contributes to Bandi et al. (2021), and related literature, by revisiting their results with a replication study and extending their spectral factor model to the corporate bond market.

The literature reviewed above primarily focuses on the US equity market, with limited research exploring the role of frequency in other asset classes. Therefore, this paper contributes significantly to existing literature by examining frequency-specific systematic risk and risk premia for corporate bonds. Only recently, literature has touched upon the role of frequency in the corporate bond market. For instance, Elkamhi et al. (2024) find that a single-factor model—with long-run consumption risk as a common factor—explains the expected excess returns on

a diverse set of corporate bond portfolios. This long-run consumption risk factor is measured by accumulating the consumption growth of wealthy households over the past 24 quarters. We deviate from Elkamhi et al. (2024) by employing the extended Wold representation introduced by Ortu et al. (2020) to construct frequency-specific factors, instead of using aggregation. This distinction is crucial to highlight. Namely, Bandi and Tamoni (2023) formalise the link between aggregation and the frequency-specific components from the extended Wold decomposition, and conclude that the former can be seen as a noisy proxy for the latter. Empirically, they show that a *business cycle component* of consumption growth, spanning a period between 4 and 8 years, yields equivalent cross-sectional pricing performance in the equity market as accumulating the growth rates over a 4-year horizon.

Moreover, this paper is motivated by the research on corporate bonds conducted by Dickerson, Mueller and Robotti (2023). They find that popular bond factor models proposed in earlier literature do not outperform the bond CAPM. For example, Bai et al. (2019) demonstrate that three novel factors—credit, liquidity, and downside risk—add incremental explanatory power beyond the bond market factor. However, Dickerson, Mueller and Robotti (2023) reveal that the four-factor model of Bai et al. (2019) (consisting of these three novel factors and the bond market factor) is not properly constructed since it consists of lead-lag errors. The main objective of Dickerson, Mueller and Robotti (2023) is to underscore the importance of transparent data collection and cleaning procedures. This is particularly critical in the context of corporate bond pricing, which involves over-the-counter transactions and lacks error-free databases, unlike equity markets. This paper follows the data collection and cleaning procedures of Dickerson, Mueller and Robotti (2023).

Therefore, this paper contributes to the recent literature that (re-)evaluates the proposed factor model for corporate bonds. First, this literature focuses on how reliable datasets of corporate bond returns could be constructed (Andreani, Palhares & Richardson, 2023; Dickerson, Mueller & Robotti, 2023). For instance, Dick-Nielsen et al. (2023) propose a novel framework to clean corporate bond data and show that most risk factors suggested in previous literature cannot be replicated using this refined dataset. Second, this literature studies the role of transaction costs in the over-the-counter corporate bond market (Ivashchenko & Kosowski, 2023).

Finally, this paper contributes to the existing literature that tries to bring order to the *factor zoo*, which refers to the overwhelming number of risk factors that have been proposed in literature, both for equity and corporate bond pricing models. For instance, Dickerson, Julliard and Mueller (2023) use a hierarchical Bayesian method to analyse 563 trillion possible corporate bond factor models. They conclude, however, that most risk factors are not priced, and only one factor is shown to be in the SDF with a high probability. Using a similar technique for equity pricing, Bryzgalova, Huang and Julliard (2023) study 2 quadrillion possible factor models. They conclude that only 23 to 25 risk factors are included in the SDF with high probability. This discussion illustrates a general problem in the asset pricing literature. A potential solution might be a decomposition of risk factors across frequencies. First, it could uncover potential hidden sources of risk, captured by the spectral betas, as well as their economic determinants (Bandi & Tamoni, 2022). In addition, from a methodological perspective, the spectral betas can be seen as the result of extracting *signal* from the *noisy* aggregate beta estimate (i.e., the beta of the

traditional factor model).

3   Methodology

In this section, we introduce the spectral factor model proposed by Bandi et al. (2021). First, we provide the intuition behind the frequency-based decomposition of a factor model in Section 3.1. Next, we formalise the construction of the frequency-specific components from the extended Wold representation in Section 3.2. Finally, we discuss the identification of the extended Wold representation for empirical applications in Section 3.3.

3.1   Spectral factor model: Intuition

In this paper, we define the *traditional* linear factor model by

$$y_t = \alpha + \beta x_t + u_t, \tag{1}$$

where y_t represents the excess asset return and x_t is the risk factor, both observed at time t. Furthermore, u_t is an error term. The spectral factor model generalises this traditional model by decomposing y_t and x_t into frequency-specific components that capture cycles of different lengths. In this way, systematic risk—captured by the frequency-specific betas—is allowed to vary over frequency.

To illustrate this spectral decomposition, let us consider the spectral factor model in a simplified context. Specifically, we assume that the risk factor (x_t) and the excess asset return (y_t) can be decomposed into two frequency-specific components, each capturing cycles with a length larger than 2^j periods (e.g., months) and smaller than 2^j periods, respectively. This means that $y_t = y_t^{<2^j} + y_t^{>2^j}$ and $x_t = x_t^{<2^j} + x_t^{>2^j}$, where the superscripts indicate the cycle length of the components in number of periods. In Section 3.2, we generalise this decomposition to more than two frequency-specific components, where the frequency-specific component at scale j captures cycles between 2^{j-1} and 2^j periods. Furthermore, the dyadic nature of the cycles is inherent to the spectral decomposition.

Another convenient feature of the decomposition is the orthogonality of the frequency-specific components of x_t and y_t, which is formalised by the following two expressions

$$\mathbb{C}\left[y_t^{<2^j}, y_t^{>2^j}\right] = 0 = \mathbb{C}\left[x_t^{<2^j}, x_t^{>2^j}\right], \tag{2}$$

$$\mathbb{C}\left[y_t^{<2^j}, x_t^{>2^j}\right] = 0 = \mathbb{C}\left[x_t^{<2^j}, y_t^{>2^j}\right]. \tag{3}$$

These equations imply that the spectral components are orthogonal both within and across series. This feature is useful, especially in the context of cross-sectional asset pricing. Following the discussion of Cochrane (2009) and Kan et al. (2013), the statistical significance of the prices of multivariate beta risk (i.e., gammas) can only be used to determine whether a factor *is priced*. However, to determine whether a (correlated) risk factor adds *incremental* cross-sectional pricing power in a multifactor model, we should use the statistical significance on the prices of covariance risk, or the prices of univariate beta risk (i.e., lambdas). However, since our spectral factors are

orthogonal—within and across processes—the univariate betas coincide with the multivariate betas.

Having constructed the orthogonal frequency-specific components of the excess asset return and the risk factor, we define the *spectral factor model* as

$$y_t = \alpha + \beta^{HF} x_t^{HF} + \beta^{LF} x_t^{LF} + u_t, \tag{4}$$

where, for ease of interpretation and notation, $x_t^{HF} = x_t^{<2^j}$ and $x_t^{LF} = x_t^{>2^j}$ are the high-frequency (HF) and low-frequency (LF) spectral component, respectively. The corresponding *spectral betas* are denoted by β^{HF} and β^{LF}. Using the expression in Eq. (2), we define these spectral betas by

$$\beta^{HF} = \frac{\mathbb{C}\left[y_t, x_t^{HF}\right]}{\mathbb{V}\left[x_t^{HF}\right]}, \tag{5}$$

$$\beta^{LF} = \frac{\mathbb{C}\left[y_t, x_t^{LF}\right]}{\mathbb{V}\left[x_t^{LF}\right]}. \tag{6}$$

Moreover, due to the orthogonality of the frequency-specific components *across* processes, as implied by Eq. (3), the expression in Eqs. (5) and (6) can be reformulated as

$$\beta^{HF} = \frac{\mathbb{C}\left[y_t^{HF}, x_t^{HF}\right]}{\mathbb{V}\left[x_t^{HF}\right]}, \tag{7}$$

$$\beta^{LF} = \frac{\mathbb{C}\left[y_t^{LF}, x_t^{LF}\right]}{\mathbb{V}\left[x_t^{LF}\right]}, \tag{8}$$

where y_t^{HF} and y_t^{LF} are the low- and high-frequency spectral components of the excess asset return, respectively. The spectral betas in Eqs. (7) and (8) are identified by the following two linear regression equations,

$$y_t^{HF} = \alpha + \beta^{HF} x_t^{HF} + u_t \quad \text{and} \quad y_t^{LF} = \alpha + \beta^{LF} x_t^{LF} + u_t.$$

It is important to emphasise that the spectral factor model defined in Eq. (4) allows systematic risk to vary over frequencies, while the traditional factor model defined in Eq. (1) implicitly assumes that the spectral betas are constant over the scales j. This observation becomes explicit when we rewrite the aggregate beta in Eq. (1) as a weighted average of the spectral betas defined in Eqs. (7) and (8) as follows

$$\begin{aligned}
\beta &= \frac{\mathbb{C}\left[y_t, x_t\right]}{\mathbb{V}\left[x_t\right]}, \\
&= \frac{\mathbb{C}\left[y_t^{HF} + y_t^{LF}, x_t^{HF} + x_t^{LF}\right]}{\mathbb{V}\left[x_t\right]}, \\
&= \frac{\mathbb{C}\left[y_t^{HF}, x_t^{HF}\right]}{\mathbb{V}\left[x_t\right]} + \frac{\mathbb{C}\left[y_t^{LF}, x_t^{LF}\right]}{\mathbb{V}\left[x_t\right]},
\end{aligned}$$

$$
= \frac{\mathbb{V}\left[x_t^{HF}\right]}{\mathbb{V}\left[x_t\right]} \frac{\mathbb{C}\left[y_t^{HF}, x_t^{HF}\right]}{\mathbb{V}\left[x_t^{HF}\right]} + \frac{\mathbb{V}\left[x_t^{LF}\right]}{\mathbb{V}\left[x_t\right]} \frac{\mathbb{C}\left[y_t^{LF}, x_t^{LF}\right]}{\mathbb{V}\left[x_t^{LF}\right]},
$$
$$
= v^{HF}\beta^{HF} + v^{LF}\beta^{LF}, \tag{9}
$$

where $v^j = \mathbb{V}[x_t^j]/\mathbb{V}[x_t]$ is the *relative variance weight* for component $j \in \{HF, LF\}$. Furthermore, we used Eqs. (2) and (3) to separate the covariance term in the second line above. Following Eq. (9), we may conclude that the traditional beta (β) is a weighted average of the spectral betas, since $v^{HF} + v^{LF} = 1$. Moreover, it is clear that the traditional factor model imposes the spectral betas to be equal to each other, $\beta^{HF} = \beta^{LF} = \beta$. Thus, it is misspecified when systematic risk is frequency-dependent, such that $\beta^{HF} \neq \beta^{LF}$. In many economic applications, the high-frequency component of x_t is likely much more volatile than the low-frequency component, which results in $v^{HF} > v^{LF}$. This implies that the high-frequency component will be weighted more heavily in the aggregate beta (see Eq. (9)), while the low-frequency spectral beta (β^{LF}) might contain an important signal for asset pricing. Therefore, the main objective of the spectral factor model is to decompose systematic risk into frequency-specific components, such that potential *signal* can be separated from *noise*.

3.2   Extended Wold representation

In this section, the construction of the orthogonal frequency-specific components of the excess asset return (y_t), and risk factor (x_t), is formalised. These processes are decomposed using the *extended Wold representation* for covariance-stationary time series introduced by Ortu et al. (2020) and Bandi et al. (2019). We continue the discussion with the bivariate process used in the previous section, $\mathbf{x} = \{(y_t, x_t)\}_{t \in \mathbb{Z}}$. This is without loss of generality since the discussion below can easily be extended to a multivariate process (see e.g., Bandi & Tamoni, 2022).

First, it is important to emphasise that the decomposition relies on the covariance-stationary property of the process $\mathbf{x}$. Specifically, a covariance-stationary process can always be presented in white noise shocks, or in other words, in its *Wold* representation (Wold, 1938). To formalise this, let us define a white noise process $\boldsymbol{\varepsilon} = \{(\varepsilon_t^1, \varepsilon_t^2)\}_{t \in \mathbb{Z}}$, with zero mean, $\mathbb{E}[\boldsymbol{\varepsilon}] = 0$, and covariance matrix given by $\boldsymbol{\Sigma}_\varepsilon = \mathbb{E}[\boldsymbol{\varepsilon}\boldsymbol{\varepsilon}^\mathsf{T}]$. Then, the Wold representation of $\mathbf{x}$ is given by

$$
\begin{pmatrix} y_t \\ x_t \end{pmatrix} = \sum_{k=0}^{\infty} \begin{pmatrix} \alpha_k^1 & \alpha_k^2 \\ \alpha_k^3 & \alpha_k^4 \end{pmatrix} \begin{pmatrix} \varepsilon_{t-k}^1 \\ \varepsilon_{t-k}^2 \end{pmatrix} = \sum_{k=0}^{\infty} \boldsymbol{\alpha}_k \boldsymbol{\varepsilon}_{t-k}, \tag{10}
$$

where $\boldsymbol{\alpha}_0$ is a 2×2 identity matrix, $\mathbf{I}_2$. Moreover, note that the expression in Eq. (10) assumes that $\mathbf{x}$ has a zero mean. However, this assumption can be relaxed by adding a constant term to the Wold representation.

Next, the Wold representation in Eq. (10) is reformulated to the *extended* Wold representation. For this, the discrete Haar transform (DHT; Haar, 1911) is used to aggregate the Wold coefficients and residuals, which results in the following two expressions.

$$
\varepsilon_t^{(j)} = \frac{1}{\sqrt{2^j}} \left(\sum_{i=0}^{2^{j-1}-1} \boldsymbol{\varepsilon}_{t-i} - \sum_{i=0}^{2^{j-1}-1} \boldsymbol{\varepsilon}_{t-2^{j-1}-i} \right), \tag{11}
$$

$$\mathbf{\Psi}_k^{(j)} = \frac{1}{\sqrt{2^j}} \left(\sum_{i=0}^{2^{j-1}-1} \boldsymbol{\alpha}_{k2^j+i} - \sum_{i=0}^{2^{j-1}-1} \boldsymbol{\alpha}_{k2^j+2^{j-1}+i} \right). \tag{12}$$

Then, the extended Wold representation of $\mathbf{x}$ is defined as

$$\begin{pmatrix} y_t \\ x_t \end{pmatrix} = \sum_{j=1}^{\infty} \sum_{k=0}^{\infty} \mathbf{\Psi}_k^{(j)} \boldsymbol{\varepsilon}_{t-k2^j}^{(j)} = \sum_{j=1}^{\infty} \mathbf{x}_t^{(j)}, \tag{13}$$

where $\mathbf{x}_t^{(j)}$ is the frequency-specific component of $\mathbf{x}$ corresponding to the jth scale. Ortu et al. (2020) shows that these *spectral components* are orthogonal across scales j.

Moreover, it can be shown that the shocks associated with $\mathbf{x}_t^{(j)}$ are white noise over the support $S_t^{(j)} = \{t - k2^j : k \in \mathbb{Z}\}$. This means that $\mathbf{x}_t^{(j)}$ itself has a Wold representation, given by $\sum_{k=0}^{\infty} \mathbf{\Psi}_k^{(j)} \boldsymbol{\varepsilon}_{t-k2^j}^{(j)}$, over the support $S_t^{(j)}$. For this reason, the spectral component of $\mathbf{x}_t$ at scale j can be interpreted as a frequency-specific factor that captures cycles with a length between 2^{j-1} and 2^j time units (Bandi et al., 2021). Furthermore, since we use monthly data in this paper, each scale is converted to its corresponding cycle length in months in Table 1.

Table 1
Conversion of frequency-scales to cycle length in months

Scale	Time horizon
$j = 1$	$1 - 2$ months
$j = 2$	$2 - 4$ months
$j = 3$	$4 - 8$ months
$j = 4$	$8 - 16$ months
$j = 5$	$16 - 32$ months
$j = 6$	$32 - 64$ months
$j > 6$	> 64 months

Following the extended Wold representation in Eq. (13), the spectral factor model is defined as

$$y_t = \alpha + \sum_{j=1}^{J} \beta^{(j)} x_t^{(j)} + \beta^{(J+1)} \pi_t^{(J)} + u_t, \tag{14}$$

where $\pi_t^{(J)} = x_t - \sum_{j=1}^{J} x_t^{(j)}$, the *residual* component. Note that this residual component is a convenient way to prevent truncation of the infinite sum in Eq. (13). Also, due to the orthogonality of the spectral components, it does not affect the spectral beta estimates.

Finally, we formalise the representation of the aggregate beta of a traditional factor model as a weighted average of spectral betas, as in Eq. (9). More specifically, we state the following theorem presented in Bandi et al. (2021), for completeness.

Theorem 3.1. *Let* $\mathbf{x} = \{(y_t, x_t)\}_{t \in \mathbb{Z}}$ *be a covariance-stationary process, and the frequency-specific beta at scale j be given by* $\beta^{(j)} = \frac{\mathbb{C}\left[y_t^{(j)}, x_t^{(j)}\right]}{\mathbb{V}\left[x_t^{(j)}\right]}$. *Then, the aggregate beta is defined as* $\beta = \frac{\mathbb{C}[y_t, x_t]}{\mathbb{V}[x_t]} = \sum_{j=1}^{\infty} v^{(j)} \beta^{(j)}$ *where* $v^{(j)} = \frac{\mathbb{V}\left[x_t^{(j)}\right]}{\mathbb{V}[x_t]}$.

Proof. See Appendix B.   □

3.3   Identification

The difference between wavelet filters and the extended Wold decomposition is that the former is a non-parametric method, while the latter defines a *data generating process* (Bandi & Tamoni, 2022). This means that the extended Wold representation needs to be identified, which is the subject of this section.

First, we generalise the bivariate process in the previous sections to a multivariate process. Without loss of generality, let $\widetilde{\mathbf{x}}_t \in \mathbb{R}^{k-1}$ contain the common risk factor in the first position, and state variables in the remaining $k-2$ positions. Again, $y_t \in \mathbb{R}$ is the excess asset return at month t. Then, we define the multivariate process by $\mathbf{x}_t = (y_t, \widetilde{\mathbf{x}}_t^\intercal)^\intercal \in \mathbb{R}^k$, which is covariance stationary and has a zero mean. The objective is to decompose this multivariate process, $\mathbf{x} = \{(y_t, \widetilde{\mathbf{x}}_t^\intercal)\}_{t \in \mathbb{Z}}$, into frequency-specific components using the extended Wold representation in Eq. (13).

Since the coefficients ($\boldsymbol{\alpha}_k$) and shocks ($\boldsymbol{\varepsilon}_t$) of the Wold representation in Eq. (10) are used as input for the *extended* Wold representation, we identify first the Wold representation of $\mathbf{x}$. For this purpose, we assume that $\mathbf{x}$ is a VAR(p) process, given by:

$$\mathbf{x}_t = A_1 \mathbf{x}_{t-1} + \cdots + A_p \mathbf{x}_{t-p} + \boldsymbol{\varepsilon}_t, \tag{15}$$

where A_i is a $k \times k$ coefficient-matrix, with $i \in \{1, \ldots, p\}$. The model in Eq. (15) should be rewritten to the Wold representation in Eq. (10). Therefore, we make use of the convenient property that the VAR(p) model can be expressed as a VAR(1), by

$$\mathbf{X}_t = A \mathbf{X}_{t-1} + U_t, \tag{16}$$

where $\mathbf{X}_t = \left(\mathbf{x}_t^\intercal, \mathbf{x}_{t-1}^\intercal, \ldots, \mathbf{x}_{t-p+1}^\intercal \right)^\intercal$, and A is the companion matrix of the VAR(p) model. Moreover, since $\mathbf{x}$ is assumed to be a covariance-stationary process, Eq. (16) can be formulated as

$$\mathbf{X}_t = \sum_{k=0}^{\infty} A^k U_{t-k},$$

for instance, by applying recursive substitution to Eq. (16). Now, we have identified the Wold representation as in Eq. (10), where $\boldsymbol{\alpha}_k = A^k$ and $\boldsymbol{\varepsilon}_{t-k} = U_{t-k}$.

Next, the Wold coefficients and shocks are used to identify the extended Wold representation in Eq. (13). Specifically, we identify the shocks, $\boldsymbol{\varepsilon}_t^{(j)}$, and coefficients, $\boldsymbol{\Psi}_k^{(j)}$, with the DHT filters in Eqs. (11) and (12), respectively. Then following the extended Wold representation in Eq. (13), the spectral component of $\mathbf{x}_t$ at scale j is defined as $\mathbf{x}_t^{(j)} = \sum_{k=0}^{\infty} \boldsymbol{\Psi}_k^{(j)} \boldsymbol{\varepsilon}_{t-k2^j}^{(j)}$.

Finally, to obtain a spectral factor that does not depend on the asset return process used (y) for estimation, we assume that y does not *Granger cause* $\widetilde{\mathbf{x}}$. Since the risk factor is the first element in $\widetilde{\mathbf{x}}_t$, the identification of its coefficients is not influenced by the returns on the test assets. Furthermore, the VAR(p) model in Eq. (15) is estimated with $p = 18$ lags. Bandi et al. (2021) also impose the Granger causality restriction, and use $p = 18$ lags, in their spectral factor models.

4   Data

4.1   Corporate bonds

We construct a dataset of monthly corporate bond data following the procedure outlined by Dickerson, Mueller and Robotti (2023).[§] While Dickerson, Mueller and Robotti (2023) analyse a sample period from July 2002 to December 2016, we extend their sample period to December 2021. Furthermore, as discussed in Section 2, recent literature has highlighted the inconsistent methodological choices, lack of error-free datasets, and replication problems in corporate bond asset pricing research (Dickerson, Mueller & Robotti, 2023; Dick-Nielsen et al., 2023). Therefore, this section aims to provide a detailed discussion of the data collection and cleaning procedure used in this paper.

4.1.1   Construction of panel data

The panel dataset of monthly corporate bond returns and characteristics is generated using two databases. First, we use the Trade Reporting and Compliance Engine (TRACE) database. TRACE contains intraday data on US corporate bond transactions, such as prices and other transaction data. After applying the data cleaning procedure discussed below, the intraday prices are converted to a monthly returns series. Moreover, we use the Mergent Fixed Income Securities Database (FISD), which contains corporate bond issue data and other characteristics. The FISD dataset is combined with the TRACE dataset (based on bond CUSIP) such that corporate bond factors, and characteristic-sorted test portfolios, can be constructed.

Analyzing corporate bond return data comes with challenges. The primary reason is the opaque nature of the corporate bond market since the transactions take place in the over-the-counter market. Therefore, before the monthly return series is constructed, the intraday price data is filtered from unreliable transactions. We apply the same filters as Dickerson, Mueller and Robotti (2023). For instance, we exclude bonds that are close to default, are not publicly traded in the US, or are illiquid. An overview of the filters is provided in Table 7 of Appendix A.

Next, we construct daily corporate bond prices by taking the value-weighted average of the cleaned intraday prices. The daily corporate bond prices are, in turn, used to obtain the monthly return series. For each bond, we calculate the return at month t using one of the following two definitions: (i) the bond return at the month t is the return between the end-of-month prices at month $t-1$ and month t, or (ii) the bond return at month t is defined as the return between the begin-of-month price and the end-of-month price at month t. These definitions ensure a corporate bond can have a valid return at month t, even if it is not traded in the over-the-counter market at the end of month $t-1$. They are implemented following Dickerson, Mueller and Robotti (2023) but are also more commonly used in the corporate bond literature (Dick-Nielsen, 2014; Dick-Nielsen et al., 2023). Furthermore, the end-of-month t price in the two definitions above is identified as the price in the last 5 trading days, where preference is given to the latest trading day available in the dataset. Moreover, the begin-of-month bond price at month t is identified as the price in the first 5 trading days, where preference is given to the

---

[§]Code to construct the dataset can be found on the authors' website: https://openbondassetpricing.com

earliest trading day at which the price is observed. Note that this implies that a valid return at month t cannot be calculated when, both: the bond is not traded in the last 5 working days of month t or month $t-1$, and the bond is not traded in the last five trading days of month t or the first 5 trading days of month t. Furthermore, definition (i) will always be preferred over definition (ii) when both options can be used to calculate the monthly return.

Finally, we use the monthly price data to get the monthly bond returns. Let $P_{i,t}$ be the trade price of corporate bond i at month t. Moreover, let $AI_{i,t}$ and $C_{i,t}$ be the accrued interest and coupon rate of bond i at month t, respectively. Then, the return for this bond at month t is defined as

$$r_{i,t} = \frac{P_{i,t} + AI_{i,t} + C_{i,t}}{P_{i,t-1} + AI_{i,t-1}} - 1.$$

In the cross-sectional pricing applications of this paper, we use excess returns, defined as $R_{i,t} = r_{i,t} - r_{f,t}$, where $r_{f,t}$ is the risk-free rate (i.e., the one-month US Treasury bill rate). All returns are in percentages.

4.1.2   Traded-factor models

To evaluate the spectral factor model for corporate bonds, we compare its cross-sectional pricing accuracy with other popular factor models, for which both traded- and nontraded-factor models are considered. However, the analysis of the spectral factor models compared to nontraded-factor models is presented in Appendix C.1. In this paper, we focus instead on the traded-factor models. We consider the same models as Dickerson, Mueller and Robotti (2023), which we introduce below.

Capital asset pricing model (CAPM). First, we consider the capital asset pricing model of Sharpe (1964) and Lintner (1975), which is often applied to equities. This single-factor model uses the value-weighted average excess return on the stock market as a risk factor (MKTS). The stock market comprises all US common stocks (i.e., with share codes 10 or 11) listed on the NYSE, AMEX, and NASDAQ. The excess returns are calculated relative to the risk-free rate, which is defined as the one-month US Treasury bill rate. Both the market factor and the risk-free rate are collected from Kenneth French's website (see Appendix A). We motivate the use of the CAPM in the corporate bond market by the recent trend to identify a common factor structure across asset classes (Dickerson, Mueller & Robotti, 2023).

Bond CAPM (CAPMB). We consider an equivalent capital asset pricing model for corporate bonds: the CAPMB. This single-factor model has the bond market factor (MKTB) as a risk factor, defined as the value-weighted average excess return on the corporate bond market. Also these returns are calculated in excess of the one-month US Treasury bill rate. We obtain MKTB using the dataset constructed in Section 4.1.1. Furthermore, we consider the CAPMB as an asset pricing model in this paper since previous literature has shown its accurate explanatory power, and we verify these findings on a novel sample period. Besides that, the CAPMB provides a natural benchmark model for its spectral version.

BBW four-factor model. This is the four-factor model introduced by Bai et al. (2019). It includes MKTB, a liquidity risk factor (LRF), a downside risk factor (DRF), and a credit risk

(a) Average excess return

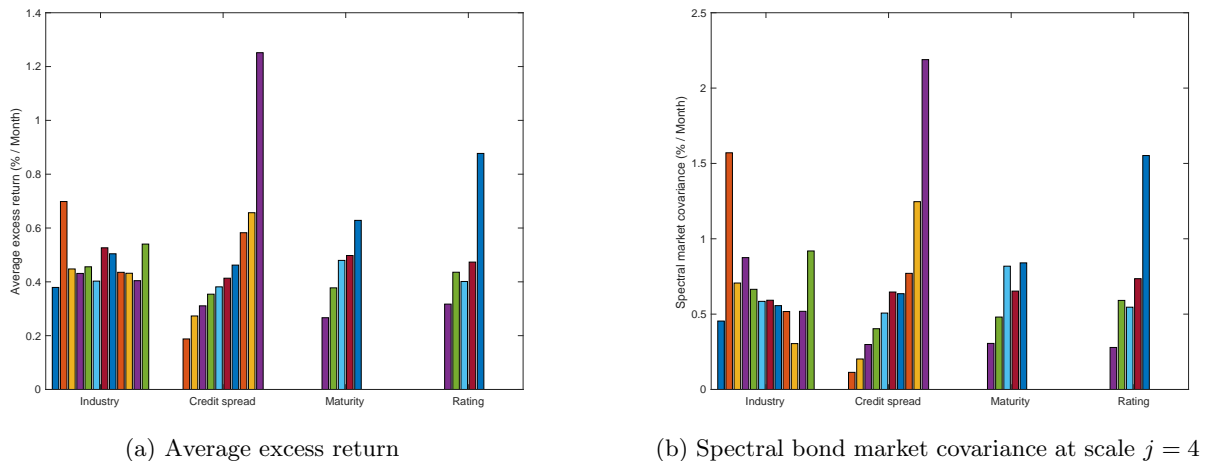(b) Spectral bond market covariance at scale $j = 4$

Figure 1: Panel (a) shows the average excess returns for the 32 test portfolios: (i) the 12 Fama-French industry portfolios; (ii) 10 portfolios sorted on credit spread; (iii) 5 portfolios sorted on maturity; and (iv) 5 portfolios sorted on rating. The sample period is from September 2008 to December 2021 (160 months). Panel (b) shows the spectral bond market covariance at scale $j = 4$ ($\widehat{\mathbb{C}}^{(4)}$).

factor (CRF). The latter three factors are constructed following a relatively complex procedure, which is discussed in Appendix A. We emphasise that the BBW risk factors were found to be inappropriately constructed (Dickerson, Mueller & Robotti, 2023). However, we use the dataset constructed in Section 4.1.1 to get the four risk factors, which are shown to be clean of lead/lag errors by Dickerson, Mueller and Robotti (2023).

Intermediary capital models (HKM/HKMSF). This is a two-factor model introduced by He et al. (2017, HKM). The model includes a factor that captures financial intermediary risk (CPTLT) and the stock market factor. The CPTLT factor is collected from the authors' website.[¶] We motivate the use of this factor model by the important role that financial intermediation has in the—over-the-counter—corporate bond market. Furthermore, He et al. (2017) show that the HKM factor model can accurately explain the cross-section of expected corporate bond return. Therefore, this paper also evaluates the single-factor model (HKMSF) that consists of only CPTLT.

Default and term-structure model (DEFTERM). This is the two-factor model introduced by Fama and French (1993). The model contains a factor that captures risk caused by changes in interest rates (TERM), and a factor that proxies the risk of default (DEF). Data on TERM and DEF is collected from Amit Goyal's website.[‖] TERM is computed as the difference between the yield on long-term US government bonds and US Treasury bills. Moreover, DEF is defined as the difference between the long-term corporate bond returns and the long-term US government bond returns. Data on the long-term government bond yield and the long-term corporate bond returns are collected from Ibbotson's *Stocks, Bonds, Bills and Inflation Yearbook*. The Treasury-bill yield in Amit Goyal's TERM variable is defined as the *1-Month Treasury Bill: Secondary Market Rate* from the Federal Reserve Economic Data (FRED) database.

[¶]See https://zhiguohe.net/data-and-empirical-patterns/

[‖]Welch and Goyal (2008) use DEF and TERM, and Amit Goyal provides updated data on these factors on his website

4.1.3   Test assets

In this paper, we use the same test portfolios as Dickerson, Mueller and Robotti (2023), which include: (i) 12 Fama-French portfolios sorted by industry classification, (ii) 10 portfolios sorted by credit spread, (iii) 5 portfolios sorted by time-to-maturity, and (iv) 5 portfolios sorted by rating. Panel (a) of Figure 1 shows the average excess portfolio returns over the sample period, revealing significant heterogeneity across the characteristic-sorted portfolios. The inclusion of the Fama-French industry portfolios is motivated by Lewellen et al. (2010). They suggest using portfolios sorted by industry since these do not have a strong common factor structure. This reduces the chances of obtaining unreasonably high ordinary least squares (OLS) cross-sectional $\mathbb{R}^2$ values in the second pass regressions, only because the proposed factors are correlated with this strong common factor structure, but do not make sense from an economic perspective. The industry portfolios are constructed by sorting corporate bonds based on groups of SIC codes, which can be extracted from Kenneth French's website (see Appendix A). Besides that, the maturity and rating portfolios are created by sorting corporate bond returns into quintiles based on time-to-maturity and bond rating, respectively. Finally, consistent with Dickerson, Mueller and Robotti (2023), the credit spread portfolios are constructed by sorting on the average credit spread between months $t-1$ and $t-12$. This one-month lag between the average credit spread measure and portfolio construction period ensures that the potential measurement errors in bond prices do not result in lead-lag effects in the return series (Elkamhi et al., 2024).

5   Results

5.1   Empirical illustration: The properties of spectral betas

In Section 3 we discussed the theoretical properties imposed by the extended Wold decomposition, such as the orthogonality of the frequency-specific components. We expect these properties to hold in an empirical application, and this section focuses on verifying them. We follow the analysis of Bandi et al. (2021) and estimate the spectral factor model on the corporate bond market.

   We start the analysis by estimating the bond CAPM (CAPMB). We consider the top and bottom quintile portfolios sorted on credit spread, which are introduced in Section 4.1. We choose these two test portfolios since they show the most heterogeneity in average excess returns in Figure 1. Let $R_{high,t}$ and $R_{low,t}$ denote the excess return at month t on the high and low credit-spread portfolios, respectively. Furthermore, let $f_{MKTB,t}$ be the bond market factor at month t. Then, the estimated CAPMB is given by

$$R_{high,t} = \alpha + 2.475 \times f_{MKTB,t} + u_t \quad \mathbb{R}^2 = 0.58, \tag{17}$$
$$(t\text{-stat} = 9.75)$$
$$R_{low,t} = \alpha + 0.314 \times f_{MKTB,t} + u_t \quad \mathbb{R}^2 = 0.53. \tag{18}$$
$$(t\text{-stat} = 5.03)$$

The CAPMBs presented above are, in turn, used to calculate the model-implied covariances between the bond market factor and the excess portfolio returns. Namely, given that the annualised volatility on the bond market factor is 6.959, the market covariance for the high credit-spread portfolio is $\widehat{\mathbb{C}}(f_{MKTB,t}, R_{high,t}) = 2.475 \times (6.959/\sqrt{12})^2 = 9.988$. Similarly, the model-implied covariance between the bond market factor and the low credit-spread portfolio return is $\widehat{\mathbb{C}}(f_{MKTB,t}, R_{low,t}) = 0.314 \times (6.959/\sqrt{12})^2 = 1.267$.

Table 2

Spectral decomposition for credit-spread-sorted portfolios. The upper panel reports the spectral covariances associated with six frequency-specific bond market factors and the corresponding frequency-components of a low and high credit spread portfolio. The lower panel reports the spectral betas and relative variance weights. The bond market factor and excess portfolio returns are decomposed into frequency-specific components using the procedure outlined in Section 3. The data are monthly from September 2008 through December 2021. The returns are in percentages.

Spectral covariances	$j=1$	$j=2$	$j=3$	$j=4$	$j=5$	$j>5$	$\sum_{j=1}^{6}\widehat{\mathbb{C}}$
High credit spread	2.342	3.753	0.681	2.202	0.542	0.408	9.929
Low credit spread	0.407	0.615	0.051	0.124	0.066	0.011	1.275

Spectral betas and weights	$j=1$	$j=2$	$j=3$	$j=4$	$j=5$	$j>5$	$\sum_{j=1}^{6}\widehat{v}^{(j)}\widehat{\beta}^{(j)}$
High credit spread	1.821	2.413	2.327	3.553	2.999	3.234	2.459
Weight (rel. variance)	0.319	0.385	0.073	0.154	0.045	0.031	
Low credit spread	0.316	0.396	0.175	0.201	0.363	0.090	0.316
Weight (rel. variance)	0.319	0.385	0.073	0.154	0.045	0.031	

Since the extended Wold decomposition can be seen as a persistence-based (co)variance decomposition method, we expect the spectral covariances to sum to the model-implied covariances presented above. The upper panel of Table 2 reports the spectral covariances, $\widehat{\mathbb{C}}(f_{MKTB}^{(j)}, R_p^{(j)})$, where $p \in \{high, low\}$. We observe that the spectral covariances for the low credit-spread portfolio sum to 1.275, which is close to the estimate (1.267) provided by the CAPMB in Eq. (18). The same holds for the high credit-spread portfolio, where the spectral covariances sum to 9.929.

Moreover, the lower panel of Table 2 reports the spectral betas ($\beta^{(j)}$) and the relative variance weights ($v^{(j)}$). Following Thereom 3.1, we expect the weighted-average of spectral betas to be equivalent to the aggregate CAPMB betas estimated in Eqs. (17) and (18), where the weights are given by $v^{(j)}$. Specifically, we expect the following expression to hold

$$\widehat{\beta} = \sum_{j=1}^{7} \widehat{v}^{(j)} \widehat{\beta}^{(j)}, \quad \text{where} \quad \widehat{v}^{(j)} = \frac{\widehat{\mathbb{V}}\left(\widehat{f}_{MKTS}^{(j)}\right)}{\widehat{\mathbb{V}}\left(\widehat{f}_{MKTS}\right)}.$$

where $\widehat{v}^{(j)}$ and $\widehat{\beta}^{(j)}$ are the relative variance weight and spectral beta at scale j, respectively. We observe in the lower panel of Table 2 that Theorem 3.1 holds, with the weighted averages of spectral betas being 2.495 and 0.316 for the high and low credit spread portfolios, respectively.

Finally, we evaluate the orthogonality of the spectral components of MKTB. Specifically, since the spectral components are orthogonal—both within and across processes—we expect that the are the same. We obtain the high-frequency components of the portfolio return and MKTB by summing the spectral components between scale $j = 1$ and $j = 3$. The sum of the three remaining spectral components define the low-frequency components. Then, we estimate

the following simple regression models

$$R_{p,t}^{HF} = \alpha + \beta_p^{HF} f_{MKTB,t}^{HF} + u_t,$$
$$R_{p,t}^{LF} = \alpha + \beta_p^{LF} f_{MKTB,t}^{LF} + u_t,$$

and the multiple regression equation

$$R_{p,t} = \alpha + \beta_p^{HF} f_{MKTB,t}^{HF} + \beta_p^{LF} f_{MKTB,t}^{LF} + u_t.$$

The resulting spectral betas are shown in Table 3. We observe that the spectral betas are very similar.

Table 3
Orthogonality of frequency-specific components of corporate bond portfolio returns. This table provides the spectral betas obtained from a simple and multiple linear regression of the high and low credit-spread-sorted portfolio excess returns on the frequency-specific components of the market excess return. The high and low credit spread portfolios are defined as the top and bottom decile portfolios obtained from sorting on credit spread. The portfolio and market (excess) returns are decomposed into six frequency-specific components (incl. the residual term $\pi^{(5)}$) using the procedure outlined in Section 3. The high-frequency (HF) component is defined as the sum of the components from scales 1 to 3 (included). By summing the three remaining components, we obtain the low-frequency (LF) component. The data are monthly from September 2008 to December 2021 (160 months). Newey-West adjusted t-statistics are reported between parentheses.

	Simple regression		Multiple regression	
	β^{LF}	β^{HF}	β^{LF}	β^{HF}
High credit spread	3.407	2.205	3.436	2.204
	(10.770)	(8.259)	(6.127)	(7.663)
Low credit spread	0.270	0.341	0.194	0.347
	(4.118)	(4.723)	(1.697)	(4.099)

5.2   Cross-sectional pricing: Corporate bonds

In this section, we explore the potential of the spectral factor model for achieving dimensionality reduction in the corporate bond factor space. We apply the spectral decomposition to the bond market factor (MKTB). Several reasons support this choice. First, unlike the CAPM in equity markets, the bond CAPM (CAPMB) is a strong factor model and, therefore, an ideal benchmark for the spectral factor model (Dickerson, Mueller & Robotti, 2023). Second, since MKTB is included in many factor models, decomposing it into frequency-specific components may offer the greatest potential for dimensionality reduction. Lastly, a frequency-based decomposition of MKTB might reveal valuable insights into its strong performance in the CAPMB.

We estimate the spectral factor models as discussed in Section 3. Given the short period on which reliable corporate bond data can be collected, we extract $J = 5$ frequency-specific components (excl. residual term, $\pi_t^{(5)}$). However, in Appendix C.2, we show that the main results are robust to setting $J = 6$. This means that we are left with a sample period from September 2008 to December 2021 (160 months).[**] The resulting frequency-specific components

---

[**]$2^J + p$ observations are needed to initialise the spectral components. The lag-length of the VAR model is set

of the bond market factor are shown in Figure 2. We observe that the components become more persistent as the scale, j, increases.
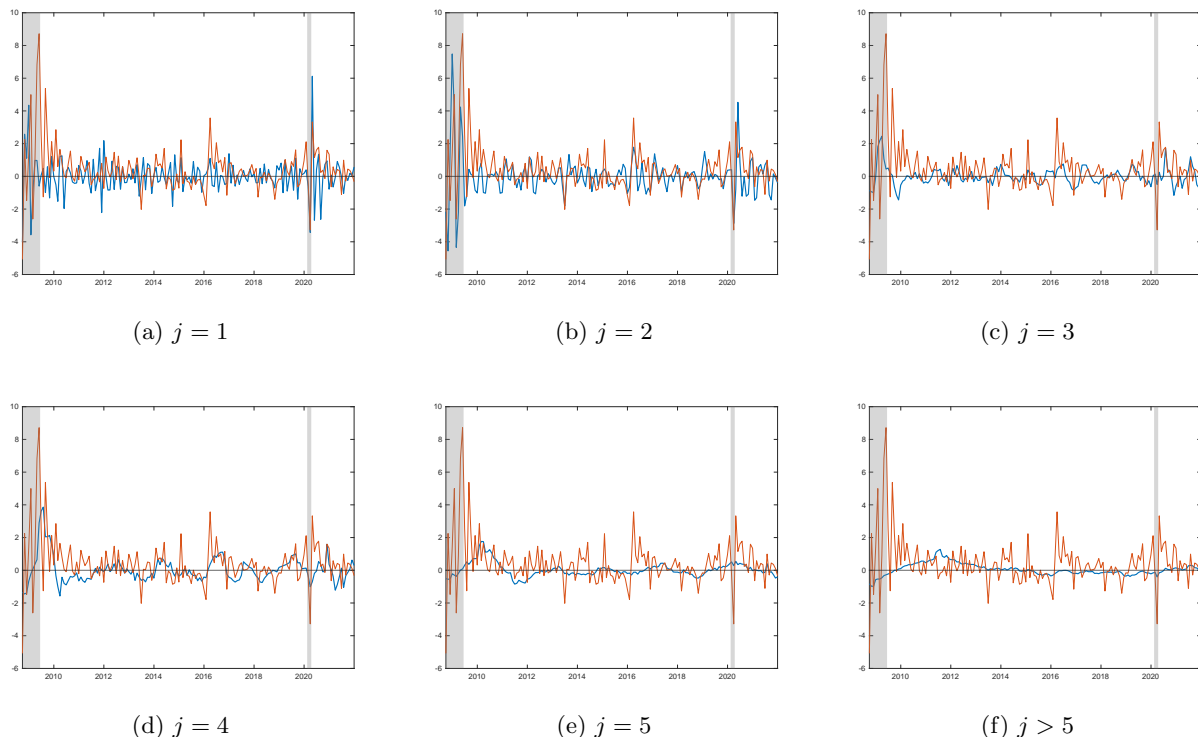

(a) $j = 1$ (b) $j = 2$ (c) $j = 3$

(d) $j = 4$ (e) $j = 5$ (f) $j > 5$

Figure 2: These figures show the spectral bond market factor for each scale j (blue). The frequency-specific components are estimated as discussed in Section 3, where J is set to 5. Furthermore, we plot the liquidity risk factor in the four-factor model of Bai et al. (2019) (orange). The sample period is from September 2008 to December 2021 (160 months). For the conversion of the scales to the cycle-length in months, see Table 1. The grey shades correspond to NBER recession periods.

Moreover, Figure 1 shows that the average excess returns on the 32 test portfolios align with the spectral market covariances for scale $j = 4$ ($\widehat{\mathbb{C}}^{(4)}$). Converting the scale to cycle length in months using Table 1, this finding suggests that an *annual cycle* component—capturing fluctuations between 8 and 16 months—may be the driving force behind the strong performance of the bond market factor.

To formally study whether the annual cycle component has indeed more pricing power than the other spectral components, and to evaluate its cross-sectional pricing accuracy compared to other factor models, we perform the second-pass regression by estimating the prices of covariance risk (i.e., lambdas, see Kan et al., 2013).[††] We define the *spectral CAPMB* as a single-factor model with the spectral bond market factor at scale $j = 4$ as a risk factor (CAPMB$^{(4)}$). The results are presented in Table 6. Besides the prices of covariance risk, the table reports the generalised method of moments (GMM) t-statistics for correctly specified models (t-stat$_c$) which account for heteroskedasticity and autocorrelation, and the model-misspecification-robust t-statistics (t-stat$_m$) of Kan et al. (2013). Also the cross-sectional R^2 values are reported in Table 6, together with p-values for the test under the null hypothesis that $R^2 = 1$ in squared brackets.

---

to $p = 18$, following Bandi et al. (2021). But the results are robust to alternative choices around $p = 18$.

[††]We should use the prices of covariance risk to determine the incremental pricing power of risk factors (except for spectral factors, Section 3.1). The prices of multivariate beta risk are presented in Table 12 of Appendix C.

We follow Dickerson, Mueller and Robotti (2023) and report both the ordinary least squares (OLS) and generalized least squares (GLS) estimates (for methodological details, see e.g., Kan et al., 2013). Lewellen et al. (2010) show that a high OLS R^2 is a relatively low hurdle when the test assets have a strong covariance structure. Therefore, the OLS R^2 is not always a good metric to evaluate asset pricing models. A solution proposed by Lewellen et al. (2010) is to report the GLS cross-sectional R^2 estimates, which are more robust to this problem.

First, we consider whether the annual cycle component of the bond market factor adds indeed incremental cross-sectional pricing power beyond the other spectral components. In Panel A of Table 6, we observe the prices of covariance risk estimated with OLS. Besides the factor models introduced in Section 4.1, this panel shows the estimates for the spectral CAPMB and a factor model including all the six spectral components. Using a 5% significance level, the annual cycle component does not add incremental pricing power to this six-factor model. However, the same conclusion is reached when considering the t-statistics of the other spectral components. In contrast, for the GLS estimates in Panel B of Table 6, only the spectral component at scale $j = 4$ possesses incremental explanatory power for the cross-sectional variation in expected returns, with values of 2.36 and 3.17 for t-stat$_c$ and t-stat$_m$, respectively. Therefore, these results confirm that the annual cycle component contains the most pricing signal.

Next, we evaluate the performance of the spectral CAPMB with the other factor models introduced in Section 4.1. First, we observe in Table 6 that the OLS and GLS R^2 estimates of the spectral CAPMB are higher than those of the CAPMB. Furthermore, the R^2 values are also higher than all the other factor models, except the four-factor model of Bai et al. (2019) (BBW) and the spectral six-factor model. To test whether these differences are statistically significant, we perform the misspecification-robust test of Kan et al. (2013) under the null-hypotheses that two different models have equal R^2. The p-values for this test, together with the differences in R^2, are reported in Table 4. The table indicates that the improvement of the spectral CAPMB over the CAPMB is not statistically significant, with p-values of 0.878 and 0.886 for the OLS and GLS R^2, respectively. The outperformance of the spectral CAPMB with respect to the other factor models is also not statistically significant. However, none of the factor models significantly outperforms another model at the 5% level.

Moreover, we compare our results to the findings of Dickerson, Mueller and Robotti (2023), who study the same factor models. First, Dickerson, Mueller and Robotti (2023) find—using a sample period from August 2004 to December 2016—that only the liquidity risk factor (LRF) in the four-factor model of Bai et al. (2019) possesses incremental pricing power. Our results in Table 6 are consistent with this finding, since LRF is the only risk factor in the BBW factor model for which its price of covariance risk is statistically significant at the 5% level. Second, Table 6 shows that the OLS and GLS R^2 for the CAPMB are 0.914 and 0.114, respectively. This means that the BBW factor model attains a higher cross-sectional fit, with an OLS R^2 of 0.938 and a GLS R^2 of 0.163. However, Table 4 indicates that these differences are not statistically significant, which is consistent with the findings of Dickerson, Mueller and Robotti (2023). Lastly, we observe in Table 6 that the CAPMB outperforms all the other factor models, which are: DEFTERM, CAPM, HKMSF, and HKM. Interestingly, some of these factor models have been shown to possess significant explanatory power for the cross-section of expected corporate

Table 4

Differences in cross-sectional (CSR) R^2 for 7 different factor models in corporate bond pricing. (i) the CAPM with the corporate bond market factor (CAMPB); (ii) the 4-factor model of Bai et al. (2019) (BBW); (iii) the Fama and French (1993) two-factor model (DEFTERM); (iv) the CAPM with the stock market factor (CAPM); (v) the single-factor intermediary capital model of He et al. (2017, HKMSF); (vi) the original two-factor model proposed by He et al. (2017, HKM), which also includes the stock market factor (MKTS); (vii) the spectral bond market factor for scale $j = 4$ (CAPMB$^{(4)}$); (viii) the spectral factor model with all 6 frequency-specific components (6 freq.). The models are estimated using monthly excess returns (in percentages) on 32 test portfolios, from 2008M9 to 2021M12. Each entry in row i and column j reports the difference in CSR R^2 between model i and model j. Misspecification-robust p-values of Kan et al. (2013), for the test under the null hypothesis of equal CSR R^2, are reported in square brackets. The normal tests are used (instead of sequential) for non-nested models.

	BBW	DEFTERM	CAPM	HKMSF	HKM	CAPMB$^{(4)}$	6 freq.
Panel A: OLS							
CAPMB	-0.024	0.065	0.037	0.063	0.032	-0.017	-0.057
	[0.906]	[0.300]	[0.752]	[0.670]	[0.751]	[0.878]	[0.482]
BBW		0.089	0.061	0.087	0.056	0.007	-0.033
		[0.281]	[0.443]	[0.440]	[0.395]	[0.929]	[0.660]
DEFTERM			-0.028	-0.002	-0.033	-0.082	-0.122
			[0.818]	[0.989]	[0.766]	[0.517]	[0.284]
CAPM				0.026	-0.005	-0.054	-0.094
				[0.594]	[0.765]	[0.510]	[0.461]
HKMSF					-0.031	-0.080	-0.120
					[0.422]	[0.332]	[0.389]
HKM						-0.049	-0.089
						[0.602]	[0.481]
CAPMB$^{(4)}$							-0.040
							[0.696]
Panel B: GLS							
CAPMB	-0.049	0.060	0.083	0.088	0.083	-0.009	-0.063
	[0.350]	[0.197]	[0.122]	[0.151]	[0.126]	[0.886]	[0.265]
BBW		0.109	0.132	0.137	0.132	0.040	-0.014
		[0.110]	[0.057]	[0.070]	[0.058]	[0.495]	[0.790]
DEFTERM			0.023	0.028	0.023	-0.069	-0.123
			[0.613]	[0.567]	[0.618]	[0.346]	[0.168]
CAPM				0.005	0.000	-0.092	-0.146
				[0.778]	[0.960]	[0.153]	[0.085]
HKMSF					-0.005	-0.097	-0.151
					[0.592]	[0.149]	[0.094]
HKM						-0.092	-0.146
						[0.153]	[0.086]
CAPMB$^{(4)}$							-0.054
							[0.828]

bond returns, such as HKM (Hou, Xue & Zhang, 2015). However, we show that these popular factor models, especially the two-factor models, cannot outperform the single-factor CAPMB and spectral CAPMB.

Given the results presented above, and the objective of this paper to achieve dimensionality reduction in the factor space, it is interesting to analyse the potential of the spectral bond market factor in crowding out other risk factors. For instance, does LRF still possess incremental explanatory power in the BBW four-factor model when the bond market factor is replaced by its annual cycle component? Table 5 presents the prices of covariance risk for this model.

Table 5

This table presents the prices of covariance risk (λ) estimated for the four-factor model of Bai et al. (2019, BBW), where the bond market factor (MKTB) is replaced by its annual cycle component. The annual cycle component of MKTB is defined as the spectral MKTB at scale $j = 4$. The model is estimated using monthly excess returns (in percentages) on 32 test portfolios, from 2008M9 to 2021M12. The t-statistics for correct (t-stat$_c$) and potentially misspecified models (Kan et al., 2013, t-stat$_m$) are in parentheses. Furthermore, p-values for the null hypothesis of $\mathbb{R}^2 = 1$ are in brackets (Kan et al., 2013). The lambdas (except λ_0) are multiplied by 100.

	Price of covariance risk				
	$\widehat{\lambda}_0$	$\widehat{\lambda}^{(4)}$	$\widehat{\lambda}_{DRF}$	$\widehat{\lambda}_{CRF}$	$\widehat{\lambda}_{LRF}$
Panel A: OLS					
Estimate	0.18	54.40	5.65	-0.18	-13.90
t-stat$_c$	(2.16)	(1.26)	(0.57)	(-0.04)	(-0.48)
t-stat$_m$	(1.85)	(1.11)	(0.40)	(-0.03)	(-0.33)
$\mathbb{R}^2$	0.941				
	[0.451]				
Panel B: GLS					
Estimate	0.05	29.67	-0.32	-0.71	15.52
t-stat$_c$	(2.33)	(2.49)	(-0.08)	(-0.22)	(1.55)
t-stat$_m$	(2.18)	(1.93)	(-0.07)	(-0.22)	(1.44)
$\mathbb{R}^2$	0.170				
	[0.003]				

Comparing the t-statistics for the risk prices in this table with the original BBW model in Table 6, we conclude that the incremental pricing power of LRF disappears when the bond market factor is replaced by its annual cycle component. Specifically, the GLS estimates in Panel B of Table 5 indicate that the risk prices of DRF, CRF and LRF are statistically insignificant at the 5% level in this adjusted BBW model. However, the spectral bond market factor is statistically significant.

To conclude, we find that dimensionality reduction in corporate bond factors models can be achieved by decomposing risk factor in the frequency domain, thereby answering our research question. Specifically, when substituting the bond market factor in the BBW factor model with its annual cycle component, the incremental explanatory power of LRF loses its statistical significance. This implies that the annual cycle component captures (at least part of) the information contained in LRF. Besides that, Figure 2 plots LRF and the spectral components of the bond market factor. The annual cycle component (i.e., $j = 4$) is highly correlated with LRF, and seems to be a slightly more persistent version. In Figure 4 of Appendix C, we observe that the correlation is almost as high as its correlation with the original bond market factor. For this reason, we term the annual cycle component as the *liquidity cycle* of the bond market factor.

Interestingly, the liquidity cycle is shorter than the business cycle ($j = 6$, see Table 1), which is consistent with previous literature. For instance, Kamara et al. (2016) find that the liquidity factor is only priced for relatively short horizons (1 to 6 months when using aggregation). Other risk factors commonly used for equities, such as value, are priced over longer horizons (2 to 3 years).

Even though, Kamara et al. (2016) study horizon-specific pricing in the equity market, the strong pricing signal of a liquidity cycle in the corporate bond market can be motivated

economically. Let us assume that business-cycle components of risk factors have the strongest signal for equities.[‡‡] Then, following Kamara et al. (2016), we would expect the components with cycles shorter than the business cycle to be important in the—over-the-counter—corporate bond market, because of its illiquidity compared to the stock market.

[‡‡]Bandi and Tamoni (2023) find that the business-cycle component of a consumption risk factor explains the cross-section of equity returns.

Table 6

This table presents the prices of covariance risk (λ) estimated under: (i) the CAPM with the corporate bond market factor (CAMPB); (ii) the 4-factor model of Bai et al. (2019) (BBW); (iii) the Fama and French (1993) two-factor model (DEFTERM); (iv) the CAPM; (v) the single-factor intermediary capital model of He et al. (2017, HKMSF); (vi) the original two-factor model proposed by He et al. (2017, HKM), which also includes the stock market factor (MKTS); (vii) the spectral CAPMB with the bond market factor at scale $j = 4$ (CAPMB$^{(4)}$); (viii) the spectral factor model with all 6 frequency-specific components (6 freq.). The models use the monthly excess returns (in percentages) on 32 test portfolios from 2008M9 to 2021M12. The t-statistics for correct (t-stat$_c$) and potentially misspecified models (Kan et al., 2013, t-stat$_m$) are in parentheses. Furthermore, p-values for the null hypothesis of $\mathbb{R}^2 = 1$ are in brackets (Kan et al., 2013). The lambdas (except λ_0) are multiplied by 100.

Panel A: Price of covariance risk (OLS)

	CAPMB		BBW					DEFTERM			CAPM		HKMSF	
	$\widehat{\lambda}_0$	$\widehat{\lambda}_{MKTB}$	$\widehat{\lambda}_0$	$\widehat{\lambda}_{MKTB}$	$\widehat{\lambda}_{DRF}$	$\widehat{\lambda}_{CRF}$	$\widehat{\lambda}_{LRF}$	$\widehat{\lambda}_0$	$\widehat{\lambda}_{DEF}$	$\widehat{\lambda}_{TERM}$	$\widehat{\lambda}_0$	$\widehat{\lambda}_{MKTS}$	$\widehat{\lambda}_0$	$\widehat{\lambda}_{CPTLT}$
Estimate	0.03	13.67	0.08	15.62	-3.83	2.04	0.60	0.16	13.62	1.78	0.28	5.59	0.37	3.50
t-stat$_c$	(0.18)	(1.59)	(1.17)	(1.04)	(-0.25)	(0.49)	(0.02)	(2.82)	(1.98)	(0.51)	(2.10)	(1.51)	(2.83)	(1.59)
t-stat$_m$	(0.17)	(1.58)	(0.84)	(0.91)	(-0.18)	(0.45)	(0.01)	(2.68)	(1.85)	(0.54)	(2.09)	(1.49)	(2.83)	(1.58)
$\mathbb{R}^2$	0.914 [0.708]		0.938 [0.387]					0.849 [0.310]			0.877 [0.455]		0.851 [0.325]	

	HKM			CAPMB$^{(4)}$		6 freq.						
	$\widehat{\lambda}_0$	$\widehat{\lambda}_{MKTS}$	$\widehat{\lambda}_{CPTLT}$	$\widehat{\lambda}_0$	$\widehat{\lambda}^{(4)}$	$\widehat{\lambda}_0$	$\widehat{\lambda}^{(1)}$	$\widehat{\lambda}^{(2)}$	$\widehat{\lambda}^{(3)}$	$\widehat{\lambda}^{(4)}$	$\widehat{\lambda}^{(5)}$	$\widehat{\lambda}^{(>5)}$
Estimate	0.23	9.14	-2.27	0.22	55.02	0.10	10.27	5.34	62.85	21.70	71.06	-162.82
t-stat$_c$	(2.08)	(1.06)	(-0.41)	(1.37)	(1.70)	(0.94)	(0.70)	(0.39)	(1.42)	(0.68)	(0.86)	(-0.93)
t-stat$_m$	(1.33)	(0.80)	(-0.30)	(1.35)	(1.69)	(0.90)	(0.68)	(0.40)	(1.30)	(0.59)	(0.76)	(-0.79)
$\mathbb{R}^2$	0.882 [0.367]			0.931 [0.779]		0.971 [0.646]						

Panel B: Price of covariance risk (GLS)

	CAPMB		BBW					DEFTERM			CAPM		HKMSF	
	$\widehat{\lambda}_0$	$\widehat{\lambda}_{MKTB}$	$\widehat{\lambda}_0$	$\widehat{\lambda}_{MKTB}$	$\widehat{\lambda}_{DRF}$	$\widehat{\lambda}_{CRF}$	$\widehat{\lambda}_{LRF}$	$\widehat{\lambda}_0$	$\widehat{\lambda}_{DEF}$	$\widehat{\lambda}_{TERM}$	$\widehat{\lambda}_0$	$\widehat{\lambda}_{MKTS}$	$\widehat{\lambda}_0$	$\widehat{\lambda}_{CPTLT}$
Estimate	0.04	13.02	0.04	12.27	-7.53	-0.14	24.74	0.05	8.45	4.40	0.05	3.37	0.05	1.93
t-stat$_c$	(2.11)	(2.08)	(1.71)	(1.13)	(-1.05)	(-0.04)	(2.72)	(2.27)	(1.86)	(1.58)	(2.45)	(1.17)	(2.64)	(1.09)
t-stat$_m$	(1.95)	(2.05)	(1.60)	(1.07)	(-1.02)	(-0.04)	(2.55)	(2.12)	(1.80)	(1.54)	(2.16)	(1.10)	(2.35)	(1.05)
$\mathbb{R}^2$	0.114 [0.004]		0.163 [0.003]					0.054 [0.000]			0.031 [0.000]		0.026 [0.000]	

	HKM			CAPMB$^{(4)}$		6 freq.						
	$\widehat{\lambda}_0$	$\widehat{\lambda}_{MKTS}$	$\widehat{\lambda}_{CPTLT}$	$\widehat{\lambda}_0$	$\widehat{\lambda}^{(4)}$	$\widehat{\lambda}_0$	$\widehat{\lambda}^{(1)}$	$\widehat{\lambda}^{(2)}$	$\widehat{\lambda}^{(3)}$	$\widehat{\lambda}^{(4)}$	$\widehat{\lambda}^{(5)}$	$\widehat{\lambda}^{(>5)}$
Estimate	0.05	3.11	0.18	0.05	44.81	0.04	1.57	11.63	8.96	33.60	56.22	-6.00
t-stat$_c$	(2.43)	(0.68)	(0.06)	(2.64)	(3.04)	(2.07)	(0.20)	(1.46)	(0.22)	(3.17)	(1.27)	(-0.08)
t-stat$_m$	(1.99)	(0.54)	(0.05)	(2.50)	(2.82)	(1.81)	(0.18)	(1.30)	(0.19)	(2.36)	(0.86)	(-0.06)
$\mathbb{R}^2$	0.031 [0.000]			0.123 [0.004]		0.177 [0.001]						

6   Conclusion

We investigate whether dimensionality reduction can be achieved in the corporate bond factor space by decomposing risk factors into orthogonal frequency-specific components. From an economic perspective, frequency-specific systematic risk may be caused by the dependence of asset returns on lagged risk factors (Kamara et al., 2016). Therefore, especially for the over-the-counter corporate bond market, where illiquidity and high trading costs lead to infrequent trading, we would expect systematic risk to be frequency-dependent. While traditional factor models restrict systematic risk to be constant across frequencies, we use the spectral factor model of Bandi et al. (2021), which relaxes this restriction. In this way, dimensionality reduction can be achieved by separating *signal* from *noise*.

We find that a spectral CAPMB with an annual cycle component of the bond market factor—capturing cycles between 8 and 16—months contains the strongest pricing signal. The OLS and GLS R^2 for this spectral CAPMB are higher than those for the traditional CAPMB and other (multi)factor models. Only the four-factor model of Bai et al. (2019) can outperform the spectral CAPMB, although the differences in R^2 are small and not statistically significant.

Interestingly, we show that only the liquidity risk factor in the four-factor model of Bai et al. (2019) possesses incremental pricing power. However, when the bond market factor is replaced by its annual cycle component in this four-factor model, the liquidity risk factor loses its incremental pricing power. This finding indicates that the annual cycle component extracts the pricing signal that is present in the liquidity risk factor. More generally, it shows that spectral factors achieve dimensionality reduction in corporate bond factor models, thereby answering our research question.

From an economic perspective, the annual cycle component can be interpreted as the liquidity cycle of the bond market factor. This conclusion is motivated by several observations. First, the annual cycle component captures (at least part of) the pricing power of the liquidity factor in the four-factor model of Bai et al. (2019). Second, the liquidity risk factor is highly correlated with the annual cycle component compared to other spectral components of the bond market factor. Lastly, also Kamara et al. (2016) find that liquidity risk is priced over the short term. However, further work should more formally study the role of liquidity and frequency in the corporate bond market.

Finally, an interesting area for future research would be the use of the spectral factor model to construct a consumption-based asset pricing model. Elkamhi et al. (2024) find that a long-term consumption risk factor—constructed by aggregating consumption growth of wealthy households over 24 months—can price the cross-section of corporate bond returns for a diverse set of test portfolios. However, it would be interesting to formally study the role of frequency in this factor model along the lines of Bandi and Tamoni (2023).

References

Amihud, Y. (2002). Illiquidity and stock returns: cross-section and time-series effects. *Journal of Financial Markets*, *5*(1), 31–56.

Andreani, M., Palhares, D. & Richardson, S. (2023). Computing corporate bond returns: a word (or two) of caution. *Review of Accounting Studies*, 1–20.

Bai, J., Bali, T. G. & Wen, Q. (2019). Common risk factors in the cross-section of corporate bond returns. *Journal of Financial Economics*, *131*(3), 619–642.

Bali, T. G., Subrahmanyam, A. & Wen, Q. (2021). The macroeconomic uncertainty premium in the corporate bond market. *Journal of Financial and Quantitative Analysis*, *56*(5), 1653–1678.

Bandi, F. M., Chaudhuri, S. E., Lo, A. W. & Tamoni, A. (2021). Spectral factor models. *Journal of Financial Economics*, *142*(1), 214–238.

Bandi, F. M., Perron, B., Tamoni, A. & Tebaldi, C. (2019). The scale of predictability. *Journal of Econometrics*, *208*(1), 120–140.

Bandi, F. M. & Tamoni, A. (2022). Spectral financial econometrics. *Econometric Theory*, *38*(6), 1175–1220.

Bandi, F. M. & Tamoni, A. (2023). Business-cycle consumption risk and asset prices. *Journal of Econometrics*, *237*(2), 105447.

Bryzgalova, S., Huang, J. & Julliard, C. (2023). Bayesian solutions for the factor zoo: we just ran two quadrillion models. *The Journal of Finance*, *78*(1), 487–557.

Chaudhuri, S. E. & Lo, A. W. (2015). Spectral analysis of stock-return volatility, correlation, and beta. In *2015 IEEE signal processing and signal processing education workshop (SP/SPE)* (pp. 232–236).

Chaudhuri, S. E. & Lo, A. W. (2018). Dynamic alpha: A spectral decomposition of investment performance across time horizons. *Management Science*, *65*(9), 4440–4450.

Chung, K. H., Wang, J. & Wu, C. (2019). Volatility and the cross-section of corporate bond returns. *Journal of Financial Economics*, *133*(2), 397–417.

Cochrane, J. (2009). *Asset pricing: Revised edition*. Princeton university press.

Cohen, R. B., Polk, C. & Vuolteenaho, T. (2009). The price is (almost) right. *The Journal of Finance*, *64*(6), 2739–2782.

Dew-Becker, I. & Giglio, S. (2016). Asset pricing in the frequency domain: theory and empirics. *The Review of Financial Studies*, *29*(8), 2029–2068.

Dickerson, A., Julliard, C. & Mueller, P. (2023). The corporate bond factor zoo. *Available at SSRN*.

Dickerson, A., Mueller, P. & Robotti, C. (2023). Priced risk in corporate bonds. *Journal of Financial Economics*, *150*(2), 103707.

Dickerson, A. & Nozawa, Y. (2024). Pricing corporate bonds with credit risk primitives. *Available at SSRN 4822379*.

Dick-Nielsen, J. (2014). How to clean enhanced trace data. *Available at SSRN 2337908*.

Dick-Nielsen, J., Feldhütter, P., Pedersen, L. H. & Stolborg, C. (2023). Corporate bond factors: replication failures and a new framework. *Available at SSRN*.

Elkamhi, R., Jo, C. & Nozawa, Y. (2024). A one-factor model of corporate bond premia. *Management Science*, *70*(3), 1875–1900.

Engle, R. F. (1978). Testing price equations for stability across spectral frequency bands. *Econometrica: Journal of the Econometric Society*, 869–881.

Fama, E. F. & French, K. R. (1993). Common risk factors in the returns on stocks and bonds. *Journal of Financial Economics*, *33*(1), 3–56.

Friedman, M. (1957). Theory of the consumption function. In *Theory of the Consumption Function*. Princeton university press.

Gençay, R., Selçuk, F. & Whitcher, B. (2003). Systematic risk and timescales. *Quantitative Finance*, *3*(2), 108.

Goldberg, M. A. & Vora, A. (1978). Bivariate spectral analysis of the capital asset pricing model. *Journal of Financial and Quantitative Analysis*, *13*(3), 435–459.

Haar, A. (1911). Zur theorie der orthogonalen funktionensysteme. *Mathematische Annalen*, *71*(1), 38–53.

Handa, P., Kothari, S. P. & Wasley, C. (1989). The relation between the return interval and betas: implications for the size effect. *Journal of Financial Economics*, *23*(1), 79–100.

Hannan, E. J. (1963a). Regression for time series. *Time Series Analysis*, 17–37.

Hannan, E. J. (1963b). Regression for time series with errors of measurement. *Biometrika*, *50*(3/4), 293–302.

Hawawini, G. (1983). Why beta shifts as the return interval changes. *Financial Analysts Journal*, *39*(3), 73–77.

He, Z., Kelly, B. & Manela, A. (2017). Intermediary asset pricing: New evidence from many asset classes. *Journal of Financial Economics*, *126*(1), 1–35.

Hou, K., Xue, C. & Zhang, L. (2015). Digesting anomalies: An investment approach. *The Review of Financial Studies*, *28*(3), 650–705.

Ivashchenko, A. & Kosowski, R. (2023). Transaction costs and capacity of systematic corporate bond strategies. *Available at SSRN 4557587*.

Jurado, K., Ludvigson, S. C. & Ng, S. (2015). Measuring uncertainty. *American Economic Review*, *105*(3), 1177–1216.

Kamara, A., Korajczyk, R. A., Lou, X. & Sadka, R. (2016). Horizon pricing. *Journal of Financial and Quantitative Analysis*, *51*(6), 1769–1793.

Kan, R., Robotti, C. & Shanken, J. (2013). Pricing model performance and the two-pass cross-sectional regression methodology. *The Journal of Finance*, *68*(6), 2617–2649.

Kang, B. U., In, F. & Kim, T. S. (2017). Timescale betas and the cross section of equity returns: Framework, application, and implications for interpreting the fama–french factors. *Journal of Empirical Finance*, *42*, 15–39.

Kelly, B., Palhares, D. & Pruitt, S. (2023). Modeling corporate bond returns. *The Journal of Finance*, *78*(4), 1967–2008.

Kothari, S. P., Shanken, J. & Sloan, R. G. (1995). Another look at the cross-section of expected stock returns. *The Journal of Finance*, *50*(1), 185–224.

Levhari, D. & Levy, H. (1977). The capital asset pricing model and the investment horizon. *The Review of Economics and Statistics*, 92–104.

Lewellen, J., Nagel, S. & Shanken, J. (2010). A skeptical appraisal of asset pricing tests. *Journal of Financial Economics*, *96*(2), 175–194.

Lin, H., Wang, J. & Wu, C. (2011). Liquidity risk and expected corporate bond returns. *Journal of Financial Economics*, *99*(3), 628–650.

Lintner, J. (1975). The valuation of risk assets and the selection of risky investments in stock portfolios and capital budgets. In *Stochastic optimization models in finance* (pp. 131–155). Elsevier.

Neuhierl, A. & Varneskov, R. T. (2021). Frequency dependent risk. *Journal of Financial Economics*, *140*(2), 644–675.

Ortu, F., Severino, F., Tamoni, A. & Tebaldi, C. (2020). A persistence-based Wold-type decomposition for stationary time series. *Quantitative Economics*, *11*(1), 203–230.

Ortu, F., Tamoni, A. & Tebaldi, C. (2013). Long-run risk and the persistence of consumption shocks. *The Review of Financial Studies*, *26*(11), 2876–2915.

Pástor, L. & Stambaugh, R. F. (2003). Liquidity risk and expected stock returns. *Journal of Political Economy*, *111*(3), 642–685.

Scholes, M. & Williams, J. (1977). Estimating betas from nonsynchronous data. *Journal of Financial Economics*, *5*(3), 309–327.

Schwartz, R. A. & Whitcomb, D. K. (1977). Evidence on the presence and causes of serial correlation in market model residuals. *Journal of Financial and Quantitative Analysis*, *12*(2), 291–313.

Sharpe, W. F. (1964). Capital asset prices: A theory of market equilibrium under conditions of risk. *The Journal of Finance*, *19*(3), 425–442.

SIFMA. (2023). *Capital markets fact book, 2023.* Retrieved from https://www.sifma.org/resources/research/fact-book/ (Accessed: 2024-06-13)

van Binsbergen, J. H., Nozawa, Y. & Schwert, M. (2023). Duration-based valuation of corporate bonds. *Jacobs Levy Equity Management Center for Quantitative Financial Research Paper*.

Welch, I. & Goyal, A. (2008). A comprehensive look at the empirical performance of equity premium prediction. *The Review of Financial Studies*, *21*(4), 1455–1508.

Wold, H. (1938). *A study in the analysis of stationary time series* (Unpublished doctoral dissertation). Almqvist & Wiksell.

A Data

In Section A.1, we describe how the risk factors for the four-factor model of Bai et al. (2019) are constructed.

A.1 BBW four-factor model

The four-factor model of Bai et al. (2019, BBW) contains a liquidity risk (LRF), downside risk (DRF), and credit risk (CRF) factor in addition to the bond market factor (MKTB). MKTB is defined as the value-weighted excess return on the corporate bond market. We discuss the construction of the other three risk factors below. The factors are constructed free of lead/lag errors by following the procedure of Dickerson, Mueller and Robotti (2023). Moreover, we do not winsorize the excess bond market returns when constructing MKTB, as in the original work of Bai et al. (2019). Dickerson, Mueller and Robotti (2023) show that this mechanically prefers multifactor models over the bond CAPM (CAPMB).

Liquidity risk factor (LRF). This risk factor for month t, LRF_t, is constructed by sorting bonds into 5×5 portfolios by rating and an illiquidity measure, in each month t. Having formed these portfolios, value-weighted long/short returns are calculated for each rating quintile, by subtracting the value-weighted return on the lowest-quintile illiquidity portfolio from the highest-quintile illiquidity portfolio. Then, LRF is the simple average of these long/short portfolios. The illiquidity measure is defined as

$$ILLIQ_t = -\mathbb{C}_t(\Delta p_{i,t,d}, \Delta p_{i,t,d+1}), \quad \text{where} \quad \Delta p_{i,t,d} = \log(P_{i,t,d}/P_{i,t,d-1}),$$

and $P_{i,t,d}$ is the price of bond i at day d of month t. Following Bai et al. (2019) and Dickerson, Mueller and Robotti (2023), $\Delta p_{i,t,d}$ can only be calculated if the number of working days between $P_{i,t,d}$ and $P_{i,t,d-1}$ is less than 8. Furthermore, $\mathbb{C}_t$ is only identified if there are at least 5 observations of $(\Delta p_{i,t,d+1}, \Delta p_{i,t,d})$ in month t. Logically, the data used to construct $ILLIQ_t$ is obtained from the panel dataset constructed in Section 4.1.

Downside risk factor (DRF). This risk factor for month t, DRF_t, is constructed by sorting bonds into 5×5 portfolios by rating and a downside risk measure, for each month t. Using these portfolios, DRF_t is defined as the simple average (across rating quintiles) of value-weighted long/short portfolio returns. For each rating quintile, the long/short portfolio return is the value-weighted return on the highest downside risk quintile-portfolio minus the value-weighted return on the lowest downside risk quintile-portfolio. Furthermore, the downside risk measure is the absolute value of a 5% value-at-risk estimate (VaR5), which is calculated using the monthly returns in the past 36 months. Similar to Dickerson, Mueller and Robotti (2023), we impose the restriction that DRF_t is only identified when a bond has a valid return for at least 24 of the 36 months.

Credit risk factor (CRF). This risk factor at time t, CRF_t is defined as the simple average on three value-weighted returns: CRF_{VaR5}, CRF_{ILLIQ} and CRF_{REV}. First, the 5×5 portfolios sorted on rating and VaR5 are used to calculate CRF_{VaR5}. Namely, for month t, CRF_{VaR5} is obtained by subtracting the value-weighted returns on the highest rating quintile-portfolios from the lowest rating quintile-portfolios. Similarly, CRF_{REV} is defined as the difference between the

value-weighted returns on the lowest rating and highest rating portfolios, from a sort on rating and short-term reversal (REV) quintiles. Finally, CRF_{ILLIQ} is defined in the same way but then from 5×5 portfolios sorted on rating and $ILLIQ$.

Table 7

This table provides an overview of the data cleaning procedure for the TRACE and FISD corporate bond databases.

Rule	Description	TRACE/FISD filter
Remove bonds that are close to default	Remove intraday bond transactions with a trade price greater than 1,000 USD or less than 5 USD	TRACE: `(rptd_pr < 1000) & (rptd_pr > 5)`
Remove bonds that do not trade on public exchanges in the US	Remove bonds issued under Rule 144A, issued through private placement, not traded in USD, and from which the issuers are not based in the US.	FISD: (1) `RULE_144A == 'N'` (2) `PRIVATE_PLACEMENT == 'N'` (3) `FOREIGN_CURRENCY == 'N'` (4) `COUNTRY_DOMICILE == 'USA'`
Remove special corporate bonds	Remove mortgage backed or asset backed bonds, equity linked or convertible bonds, structured notes, and agency backed bonds.	FISD: (1) `ASSET_BACKED == 'N'` (2) `CONVERTIBLE == 'N'` (3) `BOND_TYPE !%in% 'X'` where `'X'` == (i) Agency, muni, or government bonds: {`TXMU, CCOV, CPAS, MBS, FGOV, USTC, USBD, USNT, USSP, USSI, FGS, USBL, ABS, O30Y, O10Y, O3Y, O5Y, O4W, CCUR, O13W, O52W, O26W`} (ii) Agency-backed bonds: {`ADEB, AMTN, ASPZ, EMTN, ADNT, ARNT`
Remove bonds with a variable coupon rate		FISD: `COUPON_TYPE != 'V'`
Remove bonds with a maturity of less than one year		
Remove labelled bonds	Remove all transactions that are classified: locked-in, when-issued, or have a special sales condition.	TRACE: (1) `lckd_in_ind != 'Y'` (2) `wis_fl != 'Y'` (3) `(sale_cndtn_cd == 'None')	(sale_cndtn_cd == '@')`
Remove all trades that have a two-day settlement period or longer		TRACE: (1) `days_to_sttl_ct == '002'` (2) `days_to_sttl_ct == '001'` (3) `days_to_sttl_ct == '000'` (4) `days_to_sttl_ct == 'None'`
Remove small transactions	Remove intraday transactions with daily par volume less than 10,000 USD.	TRACE: `entrd_vol_qt >= 10000`
Remove cancelled transactions	Also adjust for transactions that are corrected or reversed.	TRACE: see Dick-Nielsen (2014).
Remove bonds with a special interest payment structure	Bonds for which the payment structure is 'N/A', 'undocumented by FISD', 'bi-monthly' and 'Variable Coupon'	FISD: `INTEREST_FREQUENCY !%in% c(-1, 13, 14, 15, 16)`
Remove bonds for accrued interest cannot be computed	Remove bonds with missing `DAY_COUNT_BASIS`, `COUPON`, `COUPON_TYPE`, `OFFERING_DATE`, `DATED_DATE` and `INTEREST_FREQUENCY`.	

B   Proof Theorem 3.1.

In this appendix, we prove Theorem 3.1, which states that the *aggregate beta* on the traditional factor model (Eq. (1)) is a linear combination of the spectral betas in the spectral factor model (Eq. (14)).

Following the theorem, we assume that $\mathbf{x} = \{(y_t, x_t)^\intercal\}_{t \in \mathbb{Z}}$ is a covariance stationary process. Furthermore, we assume that the frequency-specific beta at scale j is given by $\beta^{(j)} = \frac{\mathbb{C}[y_t^{(j)}, x_t^{(j)}]}{\mathbb{V}[x_t^{(j)}]}$. To stay within the context in which the theorem was presented, we also assume that y_t and x_t are the excess asset return and risk factor at time t, respectively. Such that the traditional factor model is given by (Eq. (1)): $y_t = \alpha + \beta x_t + u_t$.

Proof. We start the proof by deriving an expression for the aggregate beta (β). Specifically, since the traditional factor model is just a simple linear regression (Eq. (1)), where β is the slope coefficient of this equation, we use the well-known fact that

$$\beta = \frac{\mathbb{C}[y_t, x_t]}{\mathbb{V}[x_t]}. \tag{19}$$

Next, we need to prove that the β in Eq. (19) can be expressed as $\sum_{j=1}^\infty v^{(j)} \beta^{(j)}$, where $v^{(j)} = \frac{\mathbb{V}[x_t^{(j)}]}{\mathbb{V}[x_t]}$ and $\beta^{(j)}$ is the spectral beta at scale j. In order to do so, we use the assumption of Theorem 3.1 that $\mathbf{x}$ is a covariance stationary time series. Following our discussion in Section 3.2, this means that $\mathbf{x}$ can be expressed as an extended Wold representation. Thus, we use Eq. (13), and write $\mathbf{x}_t = \sum_{j=1}^\infty \mathbf{x}_t^{(j)}$, where $\mathbf{x}_t = (y_t \ x_t)^\intercal$. Then, the β in Eq. (19) can be expressed as

$$\beta = \frac{\mathbb{C}\left[\sum_{j=1}^\infty y_t^{(j)}, \sum_{p=1}^\infty x_t^{(p)}\right]}{\mathbb{V}[x_t]}, \tag{20}$$

where j and p indicate scales.

Moreover, we follow the discussion of Ortu et al. (2020), and apply the orthogonality property of $\mathbf{x}_t^{(j)}$. Specifically, we use that y_t and x_t are orthogonal to each other, and that both y_t and x_t are orthogonal *within* processes. Then, the β in Eq. (20) can be expressed as

$$\beta = \frac{\sum_{j=1}^\infty \mathbb{C}\left[y_t^{(j)}, x_t^{(j)}\right]}{\mathbb{V}[x_t]}, \tag{21}$$

since $\mathbb{C}[y_t^{(j)}, x_t^{(p)}] = 0$ for all $j \neq p$.

Finally, we use the term $v^{(j)} = \frac{\mathbb{V}[x_t^{(j)}]}{\mathbb{V}[x_t]}$, and our assumption that $\beta^{(j)} = \frac{\mathbb{C}[y_t^{(j)}, x_t^{(j)}]}{\mathbb{V}[x_t^{(j)}]}$, to reformulate Eq. (21). Specifically, we can express β as

$$\beta = \frac{1}{\mathbb{V}[x_t]} \sum_{j=1}^\infty \mathbb{C}\left[y_t^{(j)}, x_t^{(j)}\right] \cdot \frac{\mathbb{V}\left[x_t^{(j)}\right]}{\mathbb{V}\left[x_t^{(j)}\right]},$$

$$= \sum_{j=1}^\infty \beta^{(j)} \cdot \frac{\mathbb{V}\left[x_t^{(j)}\right]}{\mathbb{V}[x_t]},$$

$$= \sum_{j=1}^{\infty} \beta^{(j)} \cdot v^{(j)}.$$

In the second expression above, we used the definition of $\beta^{(j)}$, and multiplied Eq. (21) by 1 (i.e., $\frac{\mathbb{V}[x_t^{(j)}]}{\mathbb{V}[x_t^{(j)}]}$) Furthermore, to derive the third expression, we applied the definition of $v^{(j)}$.

$\square$

$$= \sum_{j=1}^{\infty} \beta^{(j)} \cdot v^{(j)}.$$

C   Additional results: Corporate bonds

In this appendix, we present additional results for the spectral factor models estimated with corporate bond returns. Specifically, in Appendix C.1, we compare the spectral CAPMB—including the annual cycle component of the bond market factor—to the nontraded-factor models. Furthermore, in Appendix C.2, we demonstrate that the results presented in this paper are robust to setting $J = 6$. We plot the annual cycle component of the bond market factor in Figure 3. The correlations between this annual cycle component and the bond market factor and liquidity risk factor (LRF) of Bai et al. (2019) are shown in Figure 4. Finally, Table 12 reports the prices of multivariate beta risk (i.e., gammas, Kan et al., 2013) for the traded-factor models in Section 5.2 and the spectral CAPMB.

C.1   Cross-sectional pricing: Nontraded-factor models

We compare the CAPMB and the spectral CAPMB (CAPMB$^{(4)}$) to nontraded-factor models. The CAPMB is the single-factor model with the bond market factor (MKTB) as a risk factor. Furthermore, the spectral CAPMB has the spectral component of MKTB at scale $j = 4$—or, in other words, its annual cycle component—as a risk factor.

We use the same nontraded factors as Dickerson, Mueller and Robotti (2023), which are introduced below. Important risk factors in the corporate bond market are usually proxied by nontraded factors, such as liquidity risk. While many studies found nontraded factors that are priced significantly in the corporate bond market, recent work by Dickerson, Mueller and Robotti (2023) reveals that most of these risk factors attain statistically insignificant risk premia. We follow the framework of Dickerson, Mueller and Robotti (2023) and evaluate these nontraded factors over a novel sample period from September 2008 to December 2021. Besides that, we compare the nontraded-factor models to the spectral CAPMB.

We conclude that these nontraded factors do not add incremental explanatory power over this novel sample period. Furthermore, the spectral CAPMB achieves a higher cross-sectional $\mathbb{R}^2$ than 2 out of the 6 factor models. However, all nontraded-factor models that we consider contain between 2 and 8 risk factors, and do not form a fair comparison for the single-factor CAPMB. Therefore, we use the model-misspecification-robust t-statistics of Kan et al. (2013), which indicate that the differences in $\mathbb{R}^2$ are not statistically significant.

The asset pricing models

First, we introduce the asset pricing models below. We discuss only the model definitions, and more details are provided by Dickerson, Mueller and Robotti (2023).

Liquidity factor models (LIQAM and LIQPS). We consider two factor models that capture liquidity risk. The first factor model (LIQAM) includes the FF3 factors introduced in Section **??**, the two risk factors of the DEFTERM model introduced in Section 4.1, and the liquidity risk measure of Amihud (2002, AM). Furthermore, the second liquidity factor model (LIQPS) is defined as LIQAM, but with the liquidity risk measure of Pástor and Stambaugh (2003, PS)

Lin, Wang and Wu (2011); Chung, Wang and Wu (2019); Bali, Subrahmanyam and Wen (2021); Elkamhi et al. (2024)

instead of AM. We use the AM and PS factors provided by Dickerson, Mueller and Robotti (2023).

Macroeconomic uncertainty factor model (MACRO) This nontraded-factor model is recently introduced by Bali et al. (2021). It includes the macroeconomic uncertainty index of Jurado, Ludvigson and Ng (2015) and MKTS. The macroeconomic uncertainty index is defined as the conditional volatility of the residual term in a forecast model for 279 macroeconomic indicators. Thus, the residual term captures unforecastable macroeconomic news, and its volatility is a proxy of macroeconomic uncertainty. The data is provided by Dickerson, Mueller and Robotti (2023), but the code to construct the time series can be found on Turan Bali's website.

Nontraded intermediary capital factor model (HKMNT). This is the nontraded-factor model of He et al. (2017), including the nontraded version of CPTLT in Section 4.1, and MKTS. These risk factors are collected from Zhigou He's website.

Volatility factor models (VOLAM and VOLPS). Finally, we consider two volatility factor models. The first factor model (VOLAM) is based on the LIQAM model introduced above, but includes also the change in the CBOE Volatility Index (VIX) as a nontraded risk factor. Similarly, the second volatility factor model (VOLPS) is equivalent to VOLAM, but with the AM liquidity risk factor substituted by PS.

Cross-sectional pricing of expected corporate bond returns

In this section, we evaluate the accuracy of the nontraded-factor models in pricing the cross-section of expected corporate bond returns. Similar to the discussion in Section 5, we report the prices of covariance risk in Table 8. Additionally, we present the prices of multivariate beta risk in Table 9. Besides the risk prices, the tables also report the cross-sectional R^2, the t-statistics under potential model misspecification (t-stat$_m$; Kan et al., 2013), and the heteroskedasticity- and autocorrelation-consistent GMM standard errors (t-stat$_c$).

First, using a 10% significance level, the model-misspecification-robust t-statistics of Kan et al. (2013) indicate that none of the nontraded risk factors is priced statistically significantly. This holds for both the prices of covariance risk (Table 8) and the prices of multivariate beta risk (Table 9). Note that this finding is consistent with Dickerson, Mueller and Robotti (2023), even though we analyse the data on a novel sample period.

Furthermore, when comparing the prices of covariance risk in Table 8 with the prices of multivariate beta risk in Table 9, we observe that the R^2 estimates are the same across tables. This can be explained by the fact that the residuals of both regression equations are the same (Kan et al., 2013). Specifically, the prices of multivariate beta risk are a linear transformation of the prices of covariance risk, $\gamma = \mathbb{V}(x_t)\lambda$, where x_t is a vector of risk factors. This holds, not only for the nontraded-factor models, but the R^2 estimates for the traded-factor models in Table 6 and Table 12 are also equivalent to each other.

Moreover, Table 10 reports the differences in cross-sectional R^2 for the spectral CAPMB and CAPMB with the nontraded-traded factor models. We observe that most of the non-traded factor models outperform the CAPMB and spectral CAPMB. However, Table 10 indicates that the differences in cross-sectional R^2 are not statistically significant, with p-values for the null-

https://sites.google.com/a/georgetown.edu/turan-bali/data-working-papers

hypothesis of equal $\mathbb{R}^2$ between 0.228 and 0.955. Also this finding is consistent with Dickerson, Mueller and Robotti (2023).

Table 8

This table presents the prices of covariance risk (λ) estimated under: (i) the macroeconomic uncertainty model of Bali et al. (2021, MACRO); (ii) the non-traded intermediary capital model of He et al. (2017, HKMNT); (iii) a 6-factor model including the liquidity risk measure of Pástor and Stambaugh (2003, LIQPS) for corporate bonds; (iv) a similar factor model as LIQPS but with liquidity risk measured as Amihud (2002, LIQAM); (v) the LIQPS factor model extended with the change in VIX as a risk factor (VOLPS); (vi) the LIQAM factor model extended with the change in VIX as a risk factor (VOLAM). The models use the monthly excess returns (in percentages) on 32 test portfolios from 2008M9 to 2021M12. The t-statistics for correct (t-stat$_c$) and potentially misspecified models (Kan et al., 2013, t-stat$_m$) are in parentheses. Furthermore, p-values for the null hypothesis of $\mathbb{R}^2 = 1$ are in brackets (Kan et al., 2013). The lambdas (except λ_0) are multiplied by 100. For conciseness, we omit the estimates for some of the risk factors.

	Panel A: Price of covariance risk (OLS)								
	MACRO			HKMNT			LIQPS		
	$\widehat{\lambda}_0$	$\widehat{\lambda}_{MKTB}$	$\widehat{\lambda}_{UNC}$	$\widehat{\lambda}_0$	$\widehat{\lambda}_{MKTS}$	$\widehat{\lambda}_{CPTL}$	$\widehat{\lambda}_0$	$\widehat{\lambda}_{MKTS}$	$\widehat{\lambda}_{PS}$
Estimate	0.14	8.59	-6.17	0.17	12.11	-4.15	0.14	6.34	-7.58
t-stat$_c$	(1.54)	(1.58)	(-0.67)	(1.87)	(1.49)	(-0.84)	(1.58)	(0.73)	(-1.33)
t-stat$_m$	(1.35)	(1.57)	(-0.67)	(1.20)	(1.33)	(-0.71)	(1.18)	(0.60)	(-0.86)
$\mathbb{R}^2$	0.944			0.894			0.925		
	[0.701]			[0.498]			[0.186]		
	LIQAM			VOLPS			VOLAM		
	$\widehat{\lambda}_0$	$\widehat{\lambda}_{MKTS}$	$\widehat{\lambda}_{AM}$	$\widehat{\lambda}_0$	$\widehat{\lambda}_{MKTS}$	$\widehat{\lambda}_{VIX}$	$\widehat{\lambda}_0$	$\widehat{\lambda}_{MKTS}$	$\widehat{\lambda}_{VIX}$
Estimate	0.15	10.35	-11.42	0.12	12.59	7.98	0.13	13.13	7.08
t-stat$_c$	(1.26)	(0.93)	(-1.47)	(1.15)	(0.95)	(1.30)	(1.35)	(0.92)	(0.67)
t-stat$_m$	(1.13)	(0.97)	(-1.56)	(1.08)	(0.96)	(1.39)	(1.32)	(0.91)	(0.60)
$\mathbb{R}^2$	0.953			0.969			0.965		
	[0.528]			[0.428]			[0.333]		
	Panel B: Price of covariance risk (GLS)								
	MACRO			HKMNT			LIQPS		
	$\widehat{\lambda}_0$	$\widehat{\lambda}_{MKTB}$	$\widehat{\lambda}_{UNC}$	$\widehat{\lambda}_0$	$\widehat{\lambda}_{MKTS}$	$\widehat{\lambda}_{CPTL}$	$\widehat{\lambda}_0$	$\widehat{\lambda}_{MKTS}$	$\widehat{\lambda}_{PS}$
Estimate	0.04	12.05	-2.79	0.05	-0.93	3.16	0.03	2.54	-2.08
t-stat$_c$	(2.15)	(2.29)	(-0.44)	(2.80)	(-0.24)	(1.11)	(1.36)	(0.57)	(-0.68)
t-stat$_m$	(2.04)	(2.28)	(-0.45)	(2.29)	(-0.19)	(0.91)	(1.24)	(0.45)	(-0.55)
$\mathbb{R}^2$	0.119			0.045			0.138		
	[0.004]			[0.001]			[0.004]		
	LIQAM			VOLPS			VOLAM		
	$\widehat{\lambda}_0$	$\widehat{\lambda}_{MKTS}$	$\widehat{\lambda}_{AM}$	$\widehat{\lambda}_0$	$\widehat{\lambda}_{MKTS}$	$\widehat{\lambda}_{VIX}$	$\widehat{\lambda}_0$	$\widehat{\lambda}_{MKTS}$	$\widehat{\lambda}_{VIX}$
Estimate	0.03	3.03	1.75	0.03	2.79	0.46	0.03	4.84	3.24
t-stat$_c$	(1.40)	(0.65)	(0.34)	(1.35)	(0.65)	(0.16)	(1.44)	(0.84)	(0.87)
t-stat$_m$	(1.26)	(0.52)	(0.33)	(1.23)	(0.53)	(0.14)	(1.30)	(0.67)	(0.59)
$\mathbb{R}^2$	0.137			0.138			0.143		
	[0.003]			[0.003]			[0.003]		

Table 9

This table presents the prices of multivariate beta risk (γ) estimated under: (i) the macroeconomic uncertainty model of Bali et al. (2021, MACRO); (ii) the non-traded intermediary capital model of He et al. (2017, HKMNT); (iii) a 6-factor model including the liquidity risk measure of Pástor and Stambaugh (2003, LIQPS) for corporate bonds; (iv) a similar factor model as LIQPS but with liquidity risk measured as Amihud (2002, LIQAM); (v) the LIQPS factor model extended with the change in VIX as a risk factor (VOLPS); (vi) the LIQAM factor model extended with the change in VIX as a risk factor (VOLAM). The models use the monthly excess returns (in percentages) on 32 test portfolios from 2008M9 to 2021M12. The t-statistics for correct (t-stat$_c$) and potentially misspecified models (Kan et al., 2013, t-stat$_m$) are in parentheses. Furthermore, p-values for the null hypothesis of $\mathbb{R}^2 = 1$ are in brackets (Kan et al., 2013). For conciseness, we omit the estimates for some of the risk factors.

Panel A: Price of beta risk (OLS)								
	MACRO			HKMNT			LIQPS		
	$\widehat{\gamma}_0$	$\widehat{\gamma}_{MKTB}$	$\widehat{\gamma}_{UNC}$	$\widehat{\gamma}_0$	$\widehat{\gamma}_{MKTS}$	$\widehat{\gamma}_{CPTL}$	$\widehat{\gamma}_0$	$\widehat{\gamma}_{MKTS}$	$\widehat{\gamma}_{PS}$
Estimate	0.14	0.42	-0.62	0.17	1.54	0.98	0.14	1.41	-0.57
t-stat$_c$	(1.54)	(2.42)	(-0.91)	(1.87)	(2.19)	(0.84)	(1.58)	(1.83)	(-1.72)
t-stat$_m$	(1.35)	(2.38)	(-0.88)	(1.20)	(2.22)	(0.75)	(1.18)	(1.80)	(-1.02)
$\mathbb{R}^2$	0.944			0.894			0.925		
	[0.701]			[0.498]			[0.186]		

	LIQAM			VOLPS			VOLAM		
	$\widehat{\gamma}_0$	$\widehat{\gamma}_{MKTS}$	$\widehat{\gamma}_{AM}$	$\widehat{\gamma}_0$	$\widehat{\gamma}_{MKTS}$	$\widehat{\gamma}_{VIX}$	$\widehat{\gamma}_0$	$\widehat{\gamma}_{MKTS}$	$\widehat{\gamma}_{VIX}$
Estimate	0.15	1.98	-0.42	0.12	1.92	-0.41	0.13	1.97	-0.39
t-stat$_c$	(1.26)	(1.83)	(-0.86)	(1.15)	(1.94)	(-0.71)	(1.35)	(2.15)	(-0.58)
t-stat$_m$	(1.13)	(2.17)	(-1.02)	(1.08)	(2.04)	(-0.71)	(1.32)	(2.30)	(-0.55)
$\mathbb{R}^2$	0.953			0.969			0.965		
	[0.528]			[0.428]			[0.333]		

Panel B: Price of beta risk (GLS)								
	MACRO			HKMNT			LIQPS		
	$\widehat{\gamma}_0$	$\widehat{\gamma}_{MKTB}$	$\widehat{\gamma}_{UNC}$	$\widehat{\gamma}_0$	$\widehat{\gamma}_{MKTS}$	$\widehat{\gamma}_{CPTL}$	$\widehat{\gamma}_0$	$\widehat{\gamma}_{MKTS}$	$\widehat{\gamma}_{PS}$
Estimate	0.04	0.52	-0.39	0.05	0.63	1.44	0.03	0.82	0.02
t-stat$_c$	(2.15)	(3.10)	(-0.85)	(2.80)	(1.22)	(1.53)	(1.36)	(1.53)	(0.08)
t-stat$_m$	(2.04)	(3.08)	(-0.86)	(2.29)	(1.15)	(1.39)	(1.24)	(1.38)	(0.07)
$\mathbb{R}^2$	0.119			0.045			0.138		
	[0.004]			[0.001]			[0.004]		

	LIQAM			VOLPS			VOLAM		
	$\widehat{\gamma}_0$	$\widehat{\gamma}_{MKTS}$	$\widehat{\gamma}_{AM}$	$\widehat{\gamma}_0$	$\widehat{\gamma}_{MKTS}$	$\widehat{\gamma}_{VIX}$	$\widehat{\gamma}_0$	$\widehat{\gamma}_{MKTS}$	$\widehat{\gamma}_{VIX}$
Estimate	0.03	0.81	0.45	0.03	0.83	-0.79	0.03	0.83	-0.65
t-stat$_c$	(1.40)	(1.52)	(1.80)	(1.35)	(1.56)	(-1.51)	(1.44)	(1.53)	(-1.37)
t-stat$_m$	(1.26)	(1.36)	(1.60)	(1.23)	(1.40)	(-1.43)	(1.30)	(1.36)	(-1.23)
$\mathbb{R}^2$	0.137			0.138			0.143		
	[0.003]			[0.003]			[0.003]		

Table 10
This table presents the differences in cross-sectional $\mathbb{R}^2$ for the spectral CAPMB (CAPMB[(4)]) and CAPMB with the nontraded-factor models introduced in the tables above. The value in row i and column j is the difference between the $\mathbb{R}^2$ of model i and j. The spectral CAPMB includes the spectral component of the bond market factor at scale $j = 4$ as a risk factor. Furthermore, we report the model-misspecification-robust p-values for the test of equal $\mathbb{R}^2$ of Kan et al. (2013) in brackets. The results are obtained using monthly excess returns (in percentages) on 32 test portfolios from September 2008 to December 2021. Finally, the OLS and GLS $\mathbb{R}^2$ estimates are reported in Panels A and B, respectively.

	MACRO	HKMNT	LIQPS	LIQAM	VOLPS	VOLAM
Panel A: OLS						
CAPMB[(4)]	-0.013	0.037	0.006	-0.022	-0.038	-0.034
	[0.832]	[0.695]	[0.948]	[0.836]	[0.647]	[0.660]
CAPMB	-0.030	0.021	-0.011	-0.039	-0.055	-0.051
	[0.499]	[0.800]	[0.837]	[0.558]	[0.453]	[0.485]
Panel B: GLS						
CAPMB[(4)]	0.004	0.078	-0.015	-0.014	-0.015	-0.020
	[0.955]	[0.238]	[0.893]	[0.892]	[0.891]	[0.837]
CAPMB	-0.005	0.069	-0.023	-0.023	-0.024	-0.029
	[0.648]	[0.291]	[0.768]	[0.753]	[0.768]	[0.684]

C.2   Robustness analysis: Six spectral components

In this appendix, we decompose the bond market factor (MKTB) into $J = 6$ frequency-specific components, as discussed in Section 3. The bond market factor is defined as the value-weighted return across all corporate bonds in excess of the one-month US Treasury bill rate (see Section 4.1).

Table 11 presents the prices of covariance risk (i.e., lambdas) estimated for a six-factor model with the spectral components between scales $j = 1$ and $j = 6$ as risk factors. We aim to determine whether the spectral component at scale $j = 4$—the annual cycle component—contains more cross-sectional pricing signal than the other components. This is assessed through the statistical significance of the prices of covariance risk, which determines the incremental explanatory power of the risk factors (Cochrane, 2009). In Panel A of Table 11, we observe the OLS estimates of the risk prices. The t-statistics under correct model specification (t-stat$_c$) that account for heteroskedasticity and autocorrelation, and under potential model misspecification (t-stat$_m$; Kan et al., 2013), indicate that the prices of covariance risk are statistically insignificant for all spectral components at the 10% significance level. However, the GLS estimates in Panel B of Table 11 indicate that the price of covariance risk is statistically significant only for the annual cycle component, thus possessing incremental cross-sectional pricing power beyond the other spectral components of MKTB.

To conclude, the annual cycle component contains the most pricing signal in the spectral factor model with six frequency-specific components of MKTB. Especially, the annual cycle component provides more signal than the *business cycle* component at scale $j = 6$. This is interesting since Elkamhi et al. (2024) obtain a consumption risk factor by aggregating consumption growth over 24 quarters. Bandi and Tamoni (2023) find that a business cycle component of consumption risk—capturing fluctuations between 4 and 8 years—achieves equivalent cross-sectional pricing power as a consumption risk factor obtained by aggregating consumption growth over a 4-year

Table 11

This table presents the prices of covariance risk (λ) for a six-factor model, which includes spectral bond market factors from scale $j = 1$ to $j = 6$. The models are estimated using monthly excess returns (in percentages) on 32 test portfolios, covering a period from 2008M9 to 2021M12. The t-statistics for correct (t-stat$_c$) and potentially misspecified models (Kan et al., 2013; t-stat$_m$) are in parentheses. Furthermore, p-values for the null hypothesis of $\mathbb{R}^2 = 1$ are in square brackets (Kan et al., 2013). The lambdas (except λ_0) are multiplied by 100.

	$\widehat{\lambda}_0$	$\widehat{\lambda}^{(1)}$	$\widehat{\lambda}^{(2)}$	$\widehat{\lambda}^{(3)}$	$\widehat{\lambda}^{(4)}$	$\widehat{\lambda}^{(5)}$	$\widehat{\lambda}^{(6)}$
Panel A: OLS							
Estimate	0.15	-25.70	-20.84	139.42	82.99	308.20	36.49
t-stat$_c$	(2.35)	(-1.14)	(-0.76)	(0.87)	(0.84)	(0.87)	(0.18)
t-stat$_m$	(1.92)	(-1.01)	(-0.48)	(0.84)	(0.77)	(0.51)	(0.09)
$\mathbb{R}^2$	0.842						
	[0.179]						
Panel B: GLS							
Estimate	0.07	-1.29	17.62	20.32	78.01	-38.76	50.26
t-stat$_c$	(4.14)	(-0.11)	(0.79)	(0.43)	(1.79)	(-0.33)	(0.54)
t-stat$_m$	(3.50)	(-0.09)	(0.67)	(0.31)	(1.81)	(-0.28)	(0.48)
$\mathbb{R}^2$	0.174						
	[0.009]						

horizon. When we translate this finding of Bandi and Tamoni (2023) to the corporate bond factor model of Elkamhi et al. (2024), the aggregation over 24 quarters might be too long for the corporate bond market. Specifically, we find that the annual cycle component contains the most cross-sectional pricing signal, and the aggregation-horizon of Elkamhi et al. (2024) would obtain a risk factor that captures risk over a cycle longer than the business cycle (Bandi & Tamoni, 2023). Future research should investigate more formally whether the aggregation horizon used by Elkamhi et al. (2024) contains the most pricing signal, using the extended Wold decomposition as in this paper.
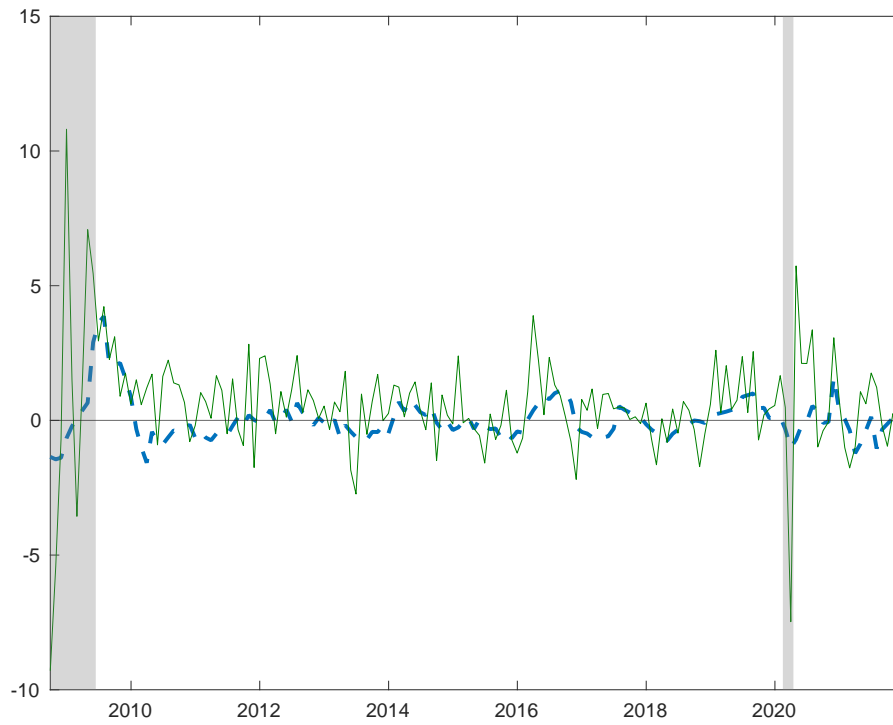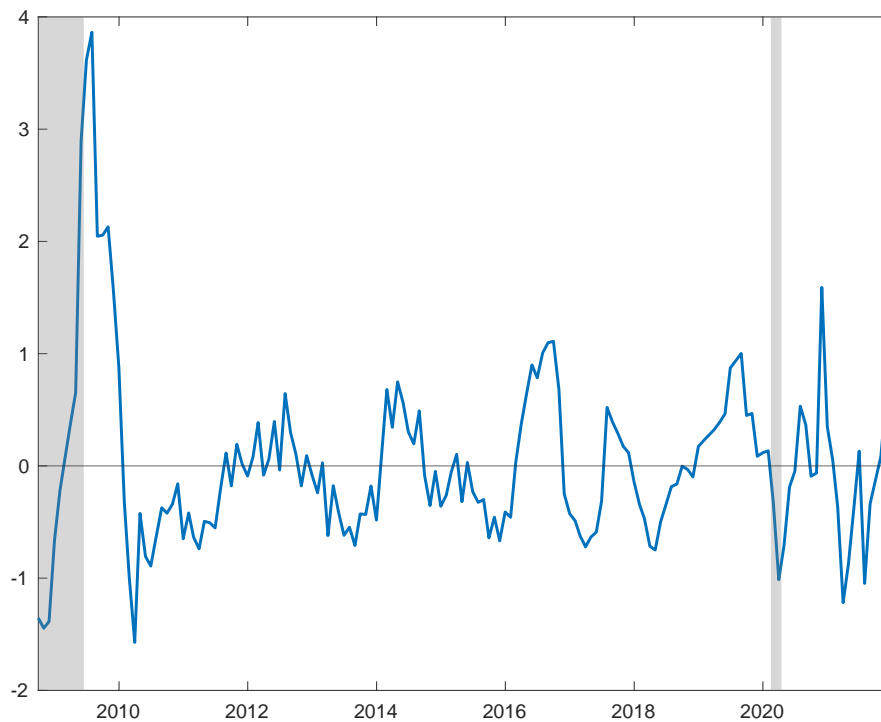
C.3   Spectral bond market factor

(a) Corporate bond market returns and cycle component at scale $j = 4$

(b) Annual cycle component at scale $j = 4$

Figure 3: The upper panel shows the spectral bond market factor at scale $j = 4$ (blue/dashed) together with the monthly market return in percentages (green). In the lower panel, we observe the spectral bond market factor at scale $j = 4$ in more detail. Monthly data is used from September 2008 to December 2021.
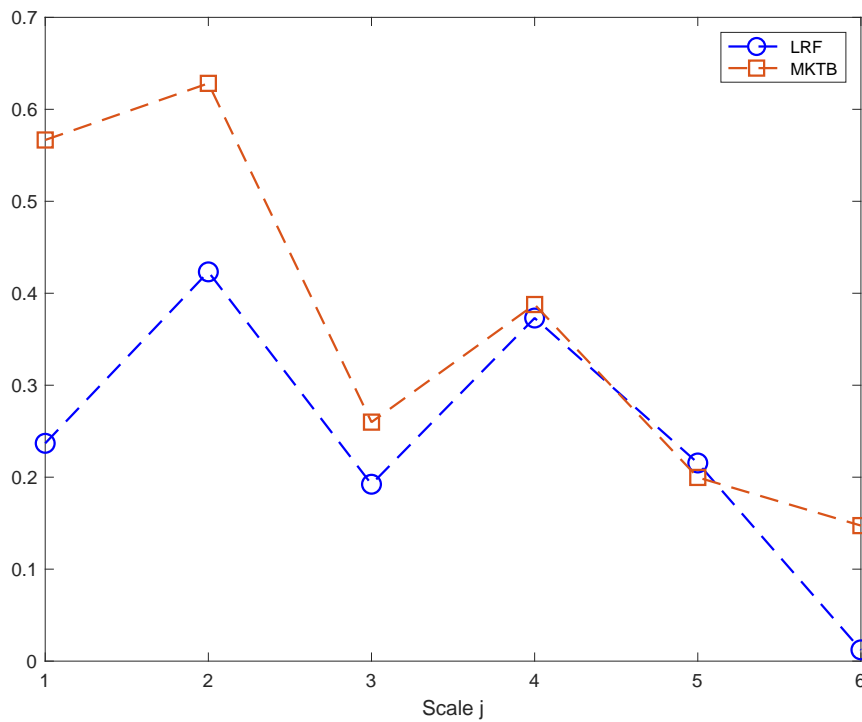
Figure 4: This figure plots the correlation for the spectral component of the bond market factor at scale j with the bond market factor (MKTB) and liquidity risk factor (LRF), respectively. LRF is the liquidity risk factor in the four-factor model of Bai et al. (2019, BBW). Furthermore, the spectral components of MKTB are constructed following the discussion in Section 3, where $J = 5$. The sample period is from September 2008 to December 2021.

Table 12

Risk premia and cross-sectional (CSR) R^2 for factor models in corporate bond pricing. The table presents the prices of multivariate beta risk (γ) estimated under: (i) the CAPM with the corporate bond market factor (CAMPB); (ii) the 4-factor model of Bai et al. (2019) (BBW); (iii) the Fama and French (1993) two-factor model (DEFTERM); (iv) the CAPM with the stock market factor (CAPM); (v) the single-factor intermediary capital model of He et al. (2017, HKMSF); (vi) the original two-factor model proposed by He et al. (2017, HKM), which also includes the stock market factor (MKTS); (vii) the spectral bond market factor for scale $j = 4$ (CAPMB$^{(4)}$); (viii) the spectral factor model with all 6 frequency-specific components (6 freq.). The models are estimated using monthly excess returns (in percentages) on 32 test portfolios, from 2008M9 to 2021M12. The t-statistics under the assumption of a correctly specified model (t-stat$_c$) and a misspecified model (Kan et al., 2013, t-stat$_m$) are provided in parentheses. Moreover, the p-values for the null of $R^2 = 1$ are provided in square brackets (Kan et al., 2013).

Panel A: Price of beta risk (OLS)

	CAPMB		BBW					DEFTERM			CAPM		HKMSF	
	$\widehat{\gamma}_0$	$\widehat{\gamma}_{MKTB}$	$\widehat{\gamma}_0$	$\widehat{\gamma}_{MKTB}$	$\widehat{\gamma}_{DRF}$	$\widehat{\gamma}_{CRF}$	$\widehat{\gamma}_{LRF}$	$\widehat{\gamma}_0$	$\widehat{\gamma}_{DEF}$	$\widehat{\gamma}_{TERM}$	$\widehat{\gamma}_0$	$\widehat{\gamma}_{MKTS}$	$\widehat{\gamma}_0$	$\widehat{\gamma}_{CPTLT}$
Estimate	0.03	0.55	0.08	0.48	0.54	0.54	0.19	0.16	0.67	-0.28	0.28	1.21	0.37	1.93
t-stat$_c$	(0.18)	(2.16)	(1.17)	(2.54)	(1.96)	(1.56)	(0.64)	(2.82)	(1.91)	(-0.57)	(2.10)	(1.79)	(2.83)	(1.70)
t-stat$_m$	(0.17)	(2.11)	(0.84)	(2.34)	(1.76)	(1.54)	(0.40)	(2.68)	(1.87)	(-0.62)	(2.09)	(1.77)	(2.83)	(1.68)
R^2	0.914		0.938					0.849			0.877		0.851	
	[0.708]		[0.387]					[0.310]			[0.455]		[0.325]	

	HKM			CAPMB$^{(4)}$		6 freq.						
	$\widehat{\gamma}_0$	$\widehat{\gamma}_{MKTS}$	$\widehat{\gamma}_{CPTLT}$	$\widehat{\gamma}_0$	$\widehat{\gamma}^{(4)}$	$\widehat{\gamma}_0$	$\widehat{\gamma}^{(1)}$	$\widehat{\gamma}^{(2)}$	$\widehat{\gamma}^{(3)}$	$\widehat{\gamma}^{(4)}$	$\widehat{\gamma}^{(5)}$	$\widehat{\gamma}^{(6)}$
Estimate	0.23	1.34	1.35	0.22	0.34	0.10	0.14	0.09	0.17	0.17	0.13	-0.21
t-stat$_c$	(2.08)	(2.00)	(1.07)	(1.37)	(1.54)	(0.94)	(0.70)	(0.46)	(1.32)	(0.78)	(0.84)	(-1.09)
t-stat$_m$	(1.33)	(1.97)	(0.92)	(1.35)	(1.53)	(0.90)	(0.71)	(0.42)	(1.10)	(0.63)	(0.79)	(-0.92)
R^2	0.882			0.931		0.971						
	[0.367]			[0.779]		[0.646]						

Panel B: Price of beta risk (GLS)

	CAPMB		BBW					DEFTERM			CAPM		HKMSF	
	$\widehat{\gamma}_0$	$\widehat{\gamma}_{MKTB}$	$\widehat{\gamma}_0$	$\widehat{\gamma}_{MKTB}$	$\widehat{\gamma}_{DRF}$	$\widehat{\gamma}_{CRF}$	$\widehat{\gamma}_{LRF}$	$\widehat{\gamma}_0$	$\widehat{\gamma}_{DEF}$	$\widehat{\gamma}_{TERM}$	$\widehat{\gamma}_0$	$\widehat{\gamma}_{MKTS}$	$\widehat{\gamma}_0$	$\widehat{\gamma}_{CPTLT}$
Estimate	0.04	0.52	0.04	0.53	0.79	0.51	0.45	0.05	0.30	0.21	0.05	0.73	0.05	1.06
t-stat$_c$	(2.11)	(3.07)	(1.71)	(3.08)	(3.02)	(1.48)	(3.23)	(2.27)	(1.50)	(0.69)	(2.45)	(1.36)	(2.64)	(1.16)
t-stat$_m$	(1.95)	(3.05)	(1.60)	(3.05)	(2.96)	(1.48)	(3.11)	(2.12)	(1.49)	(0.70)	(2.16)	(1.27)	(2.35)	(1.11)
R^2	0.114		0.163					0.054			0.031		0.026	
	[0.004]		[0.003]					[0.000]			[0.000]		[0.000]	

	HKM			CAPMB$^{(4)}$		6 freq.						
	$\widehat{\gamma}_0$	$\widehat{\gamma}_{MKTS}$	$\widehat{\gamma}_{CPTLT}$	$\widehat{\gamma}_0$	$\widehat{\gamma}^{(4)}$	$\widehat{\gamma}_0$	$\widehat{\gamma}^{(1)}$	$\widehat{\gamma}^{(2)}$	$\widehat{\gamma}^{(3)}$	$\widehat{\gamma}^{(4)}$	$\widehat{\gamma}^{(5)}$	$\widehat{\gamma}^{(6)}$
Estimate	0.05	0.73	0.98	0.05	0.28	0.04	0.02	0.18	0.02	0.21	0.10	-0.02
t-stat$_c$	(2.43)	(1.40)	(1.06)	(2.64)	(2.52)	(2.07)	(0.22)	(2.03)	(0.17)	(2.21)	(1.23)	(-0.19)
t-stat$_m$	(1.99)	(1.27)	(1.01)	(2.50)	(2.25)	(1.81)	(0.20)	(1.77)	(0.13)	(1.70)	(0.84)	(-0.14)
R^2	0.031			0.123		0.177						
	[0.000]			[0.004]		[0.001]						

D Frequency-specific betas and delayed price adjustment

Bandi et al. (2021) show that scale-varying spectral betas imply delayed price adjustments, and vice versa. In our context, a delayed price adjustment model is a model where the excess asset return (y_t) is related to lagged observations of the risk factor (x_t). We follow the analysis of Bandi et al. (2021) and provide a simple illustration that shows that delayed price adjustments imply frequency-specific betas in Appendix D.1. We extend the discussion of Bandi et al. (2021) by providing a detailed derivation, which they do not offer. Interestingly, this derivation reveals a small mistake made by Bandi and Tamoni (2022). Similarly, in Appendix D.2 we show that frequency-specific betas imply delayed price adjustments. We extend the simulation analysis of Bandi et al. (2021) by introducing a novel simulated environment, illustrating that constant spectral betas lead to the lack of delayed price adjustment in our simplified context.

D.1 Delayed price adjustments imply frequency-specific betas

In this appendix, we provide an illustration of the relationship between spectral betas and delayed adjustment models. More specifically, we show that lagged price adjustments imply frequency-specific betas (i.e., $\beta^{(j)} \neq \beta$ for all j). Assume that $\mathbf{x} = \{(y_t, x_t)^{\intercal}\}_{t \in \mathbb{Z}}$ is a covariance-stationary bivariate process. Moreover, we assume that y_t (e.g., excess return on a portfolio) is generated by a simple linear model, given by

$$y_t = \beta x_t + u_t, \tag{22}$$

where u_t is an error term with zero mean and a variance of σ_u^2. Furthermore, x_t is an AR(1) process, given by

$$x_t = \rho x_{t-1} + \varepsilon_t, \quad |\rho| < 1, \tag{23}$$

where ε_t is an error term with zero mean and a variance of σ_ε^2. The covariance between the two error terms is $\mathbb{C}(\varepsilon_t, u_t) = \sigma_{\varepsilon,u}$. We impose $|\rho| < 1$ in order to generate a covariance-stationary bivariate process $\mathbf{x}$.

The context outlined above implies a delayed adjustment of y by x when $\sigma_{\varepsilon,u} \neq 0$. This can be observed by rewriting u_t as a function of ε_t as follows

$$u_t = \frac{\sigma_{\varepsilon,u}}{\sigma_\varepsilon^2} \varepsilon_t + v_t, \tag{24}$$

where v_t is an error term with zero mean, and uncorrelated with ε_t. This formulation holds since u_t and ε_t are correlated. Moreover, we reformulate the expression in Eq. (22), using the AR(1) model for x_t in Eq. (23), as follows

$$y_t = \beta(\rho x_{t-1} + \varepsilon_t) + u_t = \beta \rho x_{t-1} + \beta \varepsilon_t + u_t, \tag{25}$$

Now, by substituting Eq. (24) in Eq. (25), we get

$$y_t = \beta x_t + \frac{\sigma_{\varepsilon,u}}{\sigma_\varepsilon^2}\varepsilon_t + v_t,$$

$$= \beta x_t + \frac{\sigma_{\varepsilon,u}}{\sigma_\varepsilon^2}(x_t - \rho x_{t-1}) + v_t,$$

$$= \left(\beta + \frac{\sigma_{\varepsilon,u}}{\sigma_\varepsilon^2}\right) x_t - \frac{\sigma_{\varepsilon,u}}{\sigma_\varepsilon^2}\rho x_{t-1} + v_t. \tag{26}$$

We observe in Eq. (26) that in our context, where $\sigma_{\varepsilon,u} \neq 0$, y is indeed a *delayed adjustment model* where the lagged factor (x_{t-1}) affects the excess return (y_t). In this situation, the spectral betas vary over the frequency components, $\{1, \dots, J\}$. Similarly, when $\sigma_{\varepsilon,u} = 0$, the model in Eq. (26) lacks delayed adjustment, and the spectral betas will be equal to the aggregate beta (i.e., $\beta^{(j)} = \beta$ for all j). An illustrative example of the spectral betas, covariances and variances, for different choices of $\sigma_{\varepsilon,u}$ and ρ, is provided in Appendix D.1.2. However, we derive first the closed-form expressions of these statistical estimators in Appendix D.1.1.

D.1.1   Derivation: spectral variances, covariances and betas

In this appendix, we derive the closed-form expressions for the spectral variances, covariances, and betas for the delayed adjustment model in Eqs. (22) and (23). A general closed-form expression for the spectral betas is provided in Appendix A.2 of Bandi et al. (2021), which we apply to our context. Furthermore, Bandi and Tamoni (2022, pp. 1201-1202) also provide the closed-form expression for the spectral betas of our delayed adjustment model, although without a derivation. Hence, we extend their analysis by offering a detailed derivation. Interestingly, this reveals a small mistake made by Bandi and Tamoni (2022).

First, for convenience, we may write the bivariate process, $\mathbf{x}$, as a VAR(1) model. Namely, using the formulations for x_t and y_t in Eq. (23) and Eq. (22), respectively, we write

$$\begin{pmatrix} y_t \\ x_t \end{pmatrix} = \begin{pmatrix} 0 & \beta\rho \\ 0 & \rho \end{pmatrix}\begin{pmatrix} y_{t-1} \\ x_{t-1} \end{pmatrix} + \begin{pmatrix} \beta\varepsilon_t + u_t \\ \varepsilon_t \end{pmatrix}$$

$$= \begin{pmatrix} 0 & \beta\rho \\ 0 & \rho \end{pmatrix}\begin{pmatrix} y_{t-1} \\ x_{t-1} \end{pmatrix} + \begin{pmatrix} \varepsilon_t^1 \\ \varepsilon_t^2 \end{pmatrix}$$

The Wold representation of this VAR(1) model is given by

$$\begin{pmatrix} y_t \\ x_t \end{pmatrix} = \sum_{k=0}^{\infty} \begin{pmatrix} 0 & \beta\rho \\ 0 & \rho \end{pmatrix}^k \begin{pmatrix} \varepsilon_{t-k}^1 \\ \varepsilon_{t-k}^2 \end{pmatrix}$$

$$= \sum_{k=1}^{\infty} \begin{pmatrix} 0 & \beta\rho^k \\ 0 & \rho^k \end{pmatrix}\begin{pmatrix} \varepsilon_{t-k}^1 \\ \varepsilon_{t-k}^2 \end{pmatrix} + \begin{pmatrix} 1 & 0 \\ 0 & 1 \end{pmatrix}\begin{pmatrix} \varepsilon_t^1 \\ \varepsilon_t^2 \end{pmatrix}$$

$$= \sum_{k=0}^{\infty} \begin{pmatrix} \alpha_k^1 & \alpha_k^2 \\ \alpha_k^3 & \alpha_k^4 \end{pmatrix}\begin{pmatrix} \varepsilon_{t-k}^1 \\ \varepsilon_{t-k}^2 \end{pmatrix} \tag{27}$$

$$= \sum_{k=0}^{\infty} \boldsymbol{\alpha}_k \boldsymbol{\varepsilon}_{t-k}$$

where we emphasise that $\boldsymbol{\alpha}_0$ is, thus, a 2×2 identity matrix, $\mathbf{I}_2$. Moreover, we observe that $\mathbb{E}[\boldsymbol{\varepsilon}_t] = \mathbf{0}$, such that the covariance matrix of the error terms can be formulated as

$$
\begin{aligned}
\boldsymbol{\Sigma}_{\boldsymbol{\varepsilon}} &= \mathbb{E}\left[\boldsymbol{\varepsilon}_t \boldsymbol{\varepsilon}_t^{\mathsf{T}}\right] \\
&= \begin{pmatrix} \sigma_u^2 + \beta^2 \sigma_\varepsilon^2 + 2\beta\sigma_{\varepsilon,u} & \sigma_{\varepsilon,u} + \beta\sigma_\varepsilon^2 \\ \bullet & \sigma_\varepsilon^2 \end{pmatrix}
\end{aligned}
\tag{28}
$$

This constant covariance matrix (over t), and the constant mean of the bivariate error term, $\boldsymbol{\varepsilon}_t$, are properties of the covariance stationary VAR(1) process.

The coefficient matrix defined in Eq. (27), and the covariance matrix in Eq. (28), are used to derive the closed-form expression for the spectral betas, $\beta^{(j)}$. Furthermore, we use the closed-form expression of a general spectral beta in Appendix A.2 of Bandi et al. (2021). Bandi and Tamoni (2022, pp. 1201-1202) also provide an expression for the spectral betas. We will show that this expression contains a small mistake. Following the notation in Bandi and Tamoni (2022), define

$$
\begin{aligned}
a_j &= \sum_{i=1}^{2^{j-1}} \rho^{i-1} \\
b_j &= a_j(1 - \rho^{2^{j-1}}) \\
c_j &= \sum_{i=0}^{2^{j-1}-1} \rho^i \\
d_j &= \rho(c_j - \rho^{2^{j-1}-1} - (\rho^{2^{j-1}-1})c_j)
\end{aligned}
$$

First, consider the variance of the spectral component $x_t^{(j)}$.

$$
\begin{aligned}
\mathbb{V}\left[x_t^{(j)}\right] &= \sum_{k=0}^{\infty} \sigma_{\varepsilon 1}^2 \left(\sum_{i=0}^{2^{j-1}-1} \alpha_{k2^j+i}^3 - \sum_{i=0}^{2^{j-1}-1} \alpha_{k2^j+2^{j-1}+i}^3\right)^2 \bigg/ 2^j \\
&\quad + \sum_{k=0}^{\infty} \sigma_{\varepsilon 2}^2 \left(\sum_{i=0}^{2^{j-1}-1} \alpha_{k2^j+i}^4 - \sum_{i=0}^{2^{j-1}-1} \alpha_{k2^j+2^{j-1}+i}^4\right)^2 \bigg/ 2^j \\
&\quad + \sum_{k=0}^{\infty} 2\sigma_{\varepsilon 1,2} \left(\sum_{i=0}^{2^{j-1}-1} \alpha_{k2^j+i}^3 - \sum_{i=0}^{2^{j-1}-1} \alpha_{k2^j+2^{j-1}+i}^3\right) \times \\
&\qquad\qquad \left(\sum_{i=0}^{2^{j-1}-1} \alpha_{k2^j+i}^4 - \sum_{i=0}^{2^{j-1}-1} \alpha_{k2^j+2^{j-1}+i}^4\right) \bigg/ 2^j
\end{aligned}
\tag{29}
$$

Using the coefficient matrix of the Wold decomposition in Eq. (27) and the covariance matrix

in Eq. (28), we can rewrite this expression to

$$\mathbb{V}\left[x_t^{(j)}\right] = 0 + \sum_{k=0}^{\infty} \sigma_\varepsilon^2 \left(\sum_{i=0}^{2^{j-1}-1} \rho^{k2^j+i} - \sum_{i=0}^{2^{j-1}-1} \rho^{k2^j+2^{j-1}+i} \right)^2 \bigg/ 2^j + 0. \tag{30}$$

The first term in Eq. (29) is zero because $\alpha_k^3 = 0$ for all k, such that the term in brackets is zero. The second term in Eq. (30) follows from the fact that $\sigma_{\varepsilon^2}^2 = \sigma_\varepsilon^2$ (see Eq. (28)), and because $\alpha_k^4 = \rho^k$ for all $k > 0$ (see Eq. (27)). Besides that, we do not need to take into account the special case of k being zero ($\boldsymbol{\alpha}_0 = \mathbf{I}_2$), because $\rho^0 = 1 = \alpha_0^4$. Moreover, the third term in Eq. (29) is zero since, again, $\alpha_k^3 = 0$ for all k. We can rewrite the variance of the jth spectral component in Eq. (30) to

$$\mathbb{V}\left[x_t^{(j)}\right] = \sigma_\varepsilon^2 \left(1 - \rho^{2^{j-1}} \right)^2 \left(\sum_{i=0}^{2^{j-1}-1} \rho^i \right)^2 \sum_{k=0}^{\infty} \left(\rho^{k2^j} \right)^2 \bigg/ 2^j$$

$$= \sigma_\varepsilon^2 b_j^2 \frac{1}{1 - \rho^{2 \cdot 2^j}} \bigg/ 2^j \tag{31}$$

This shows also immediately one of the mistakes made in Bandi and Tamoni (2022, pp. 1201-1202), where $\frac{1}{1-\rho^{4 \cdot j}}$ is written instead of $\frac{1}{1-\rho^{2 \cdot 2^j}}$ in Eq. (31).

In this second part of the derivation, we examine the covariance between the regressor $(x_t^{(j)})$ and the regressand $(y_t^{(j)})$

$$\mathbb{C}\left(y_t^{(j)}, x_t^{(j)}\right) = \mathbb{E}\left[y_t^{(j)}, x_t^{(j)}\right]$$

$$= \sum_{k=0}^{\infty} \sigma_{\varepsilon^1}^2 \left(\sum_{i=0}^{2^{j-1}-1} \alpha_{k2^j+i}^1 - \sum_{i=0}^{2^{j-1}-1} \alpha_{k2^j+2^{j-1}+i}^1 \right) \left(\sum_{i=0}^{2^{j-1}-1} \alpha_{k2^j+i}^3 - \sum_{i=0}^{2^{j-1}-1} \alpha_{k2^j+2^{j-1}+i}^3 \right) \bigg/ 2^j$$

$$+ \sum_{k=0}^{\infty} \sigma_{\varepsilon^2}^2 \left(\sum_{i=0}^{2^{j-1}-1} \alpha_{k2^j+i}^2 - \sum_{i=0}^{2^{j-1}-1} \alpha_{k2^j+2^{j-1}+i}^2 \right) \left(\sum_{i=0}^{2^{j-1}-1} \alpha_{k2^j+i}^4 - \sum_{i=0}^{2^{j-1}-1} \alpha_{k2^j+2^{j-1}+i}^4 \right) \bigg/ 2^j$$

$$+ \sum_{k=0}^{\infty} \sigma_{\varepsilon^{1,2}} \left(\sum_{i=0}^{2^{j-1}-1} \alpha_{k2^j+i}^1 - \sum_{i=0}^{2^{j-1}-1} \alpha_{k2^j+2^{j-1}+i}^1 \right) \left(\sum_{i=0}^{2^{j-1}-1} \alpha_{k2^j+i}^4 - \sum_{i=0}^{2^{j-1}-1} \alpha_{k2^j+2^{j-1}+i}^4 \right) \bigg/ 2^j$$

$$+ \sum_{k=0}^{\infty} \sigma_{\varepsilon^{1,2}} \left(\sum_{i=0}^{2^{j-1}-1} \alpha_{k2^j+i}^2 - \sum_{i=0}^{2^{j-1}-1} \alpha_{k2^j+2^{j-1}+i}^2 \right) \left(\sum_{i=0}^{2^{j-1}-1} \alpha_{k2^j+i}^3 - \sum_{i=0}^{2^{j-1}-1} \alpha_{k2^j+2^{j-1}+i}^3 \right) \bigg/ 2^j$$

Which can be rewritten to

$$
\mathbb{C}\left(y_t^{(j)}, x_t^{(j)}\right) = 0
$$

$$
+ \left[\sigma_\varepsilon^2 \left(\sum_{i=1}^{2^{j-1}-1} \beta\rho^i - \sum_{i=0}^{2^{j-1}-1} \beta\rho^{2^{j-1}+i} \right) \left(\sum_{i=0}^{2^{j-1}-1} \rho^i - \sum_{i=0}^{2^{j-1}-1} \rho^{2^{j-1}+i} \right) + \right.
$$

$$
\sum_{k=1}^{\infty} \sigma_\varepsilon^2 \left(\sum_{i=0}^{2^{j-1}-1} \beta\rho^{k2^j+i} - \sum_{i=0}^{2^{j-1}-1} \beta\rho^{k2^j+2^{j-1}+i} \right) \times
$$

$$
\left. \left(\sum_{i=0}^{2^{j-1}-1} \rho^{k2^j+i} - \sum_{i=0}^{2^{j-1}-1} \rho^{k2^j+2^{j-1}+i} \right) \right] \Bigg/ 2^j
$$

$$
+ (\sigma_{\varepsilon,u} + \beta\sigma_\varepsilon^2) \left(\sum_{i=0}^{2^{j-1}-1} \rho^{k2^j+i} - \sum_{i=0}^{2^{j-1}-1} \rho^{k2^j+2^{j-1}+i} \right) \Bigg/ 2^j \quad + \quad 0
$$

(32)

The first term in Eq. (32) is zero because $\alpha_k^3 = 0$ for all k. For the second term in Eq. (32), we used that $\sigma_{\varepsilon^2}^2 = \sigma_\varepsilon^2$ (see Eq. (28)), and we separated the case when $k = 0$ ($\alpha_0^2 = 0$ and $\alpha_0^4 = 1$) and $k \neq 0$ ($\alpha_k^2 = \beta\rho^k$ and $\alpha_k^4 = \rho^k$). However, since $\rho^0 = 1 = \alpha_0^4$, we do not need to worry about the restriction $\boldsymbol{\alpha}_0 = \mathbf{I}_2$ for α_k^4. This does not hold for α_k^2, where $\beta\rho^0 = \beta \neq \alpha_0^2$. Moreover, the third term in Eq. (32) is derived from the fact that $\sigma_{\varepsilon^{1,2}} = \sigma_{\varepsilon,u} + \beta\sigma_\varepsilon^2$ (see Eq. (28)), $\alpha_0^1 = 1$, and $\alpha_k^1 = 0$ for all $k > 0$ (see Eq. (27)). Lastly, the final term in Eq. (32) is zero because, again, $\alpha_k^3 = 0$ for all k. We may reformulate Eq. (32) to

$$
\mathbb{C}\left(y_t^{(j)}, x_t^{(j)}\right) = \left[\sigma_\varepsilon^2 \beta\rho \left(\sum_{i=0}^{2^{j-1}-1} \rho^i - \rho^{2^{j-1}-1} - \rho^{2^{j-1}-1} \sum_{i=0}^{2^{j-1}-1} \rho^i \right) b_j \right.
$$

$$
+ \sigma_\varepsilon^2 \beta \left(\sum_{i=0}^{2^{j-1}-1} \rho^i - \sum_{i=0}^{2^{j-1}-1} \rho^{2^{j-1}+i} \right)^2 \sum_{k=1}^{\infty} \left(\rho^{k2^j} \right)^2
$$

$$
\left. + (\sigma_{\varepsilon,u} + \beta\sigma_\varepsilon^2) b_j \right] \Bigg/ 2^j
$$

$$
= \left[\sigma_\varepsilon^2 \beta\rho \left(c_j - \rho^{2^{j-1}-1} - \rho^{2^{j-1}-1} c_j \right) b_j + \sigma_\varepsilon^2 \beta b_j^2 \left(\frac{1}{1-\rho^{2\cdot2^j}} - 1 \right) + \left(\sigma_{\varepsilon,u} + \beta\sigma_\varepsilon^2 \right) b_j \right] \Bigg/ 2^j
$$

$$
= \left[\sigma_\varepsilon^2 \beta\rho d_j b_j + \sigma_\varepsilon^2 \beta b_j^2 \left(\frac{1}{1-\rho^{2\cdot2^j}} - 1 \right) + \left(\sigma_{\varepsilon,u} + \beta\sigma_\varepsilon^2 \right) b_j \right] \Bigg/ 2^j
$$

(33)

In equation above, we observe that also the covariance between the spectral regressor and regressand is not correctly expressed in Bandi and Tamoni (2022, pp. 1201-1202). More specifically, the use $\left(\frac{1}{1-\rho^{4\cdot j}} - 1 \right)$ instead of $\left(\frac{1}{1-\rho^{2\cdot2^j}} - 1 \right)$.

In the final part of our derivation, we combine the variance in Eq. (31) and the covariance in Eq. (33) into a closed-form expression for the spectral betas. This expression is given by

$$
\beta^{(j)} = \frac{\mathbb{C}\left(y^{(j)}, x^{(j)}\right)}{\mathbb{V}\left(x^{(j)}\right)} = \frac{\sigma_\varepsilon^2 \beta\rho d_j b_j + \sigma_\varepsilon^2 \beta b_j^2 \left(\frac{1}{1-\rho^{2\cdot2^j}} - 1 \right) + \left(\sigma_{\varepsilon,u} + \beta\sigma_\varepsilon^2 \right) b_j}{\sigma_\varepsilon^2 b_j^2 \frac{1}{1-\rho^{2\cdot2^j}}}
$$

(34)

D.1.2   Illustration

In this appendix, we illustrate the delayed adjustment of excess asset returns (y_t) to risk factors (x_t) leads to scale-varying spectral betas. But also that the lack of delayed adjustment leads to constant spectral betas across scales. For this, we continue using the setting discussed above. Specifically, y_t is defined as in Eq. (22) and x_t as in Eq. (23). Then, the delayed adjustment model is presented in Eq. (26). We observe that if $\sigma_{\varepsilon,u} \neq 0$ (and $\rho \neq 0$), then the excess asset return is affected by a delayed component of the risk factor (x_{t-1}). The spectral betas for this delayed adjustment model in Eq. (26), also indicate that in this situation the spectral are scale-varying. Moreover, Eq. (26) also shows that when there is no delayed adjustment (i.e., either $\sigma_{\varepsilon,u} = 0$ or $\rho = 0$), then the spectral betas are constant across scales. We analyse whether this indeed holds in a simulation example below.

Specifically, we assume that $\rho = 0.5$, $\sigma_\varepsilon = 1$ and $\sigma_u = 1$. We consider different choices for $\sigma_{\varepsilon,u}$ and discuss the pattern that emerges in the resulting spectral betas. Figure 5 presents the spectral betas, spectral covariances, and spectral variances when $\sigma_{\varepsilon,u} = 0.3 > 0$ (Panel (a)), when $\sigma_{\varepsilon,u} = 0$ (Panel (b)), and when $\sigma_{\varepsilon,u} = -0.3 < 0$ (Panel (c)). The estimates are obtained following the derivation in Appendix D.1.1.

First, when $\sigma_{\varepsilon,u} > 0$, the delayed adjustment model in Eq. (26) indicates that the lagged risk factor (x_{t-1}) has a negative effect on the excess asset return (y_t), since ρ is also positive. Intuitively, we would expect that this leads to smaller estimates of systematic risk over longer horizons. For instance, when a large negative shock occurs at time t, then y_t will be negatively affected at time t, but already converge back at time $t+1$. Similarly, a large positive shock in the risk factor will positively affect y_t at time t, but y, reverts back at time $t+1$ due to the negative dependence on the lagged risk factor. Panel (a) of Figure 5 shows that the spectral betas decrease as the scale, j, increases. Therefore, since a higher scale is associated with a lower frequency or longer horizon, this figure corresponds with our intuition.

Second, when $\sigma_{\varepsilon,u} = 0$, then the delayed adjustment model in Eq. (26) shows that the excess asset return is not affected by the lagged risk factor. Specifically, Eq. (26) can be rewritten to $y_t = \beta x_t + v_t$, which is just a traditional linear factor model. Therefore, we would hope that also the spectral betas are constant across frequencies, such that the spectral betas and aggregate beta on the traditional factor model coincide (see Theorem 3.1). In Panel (b) of Figure 5, we observe the spectral betas and spectral (co)variances in this situation of no lagged dependence on risk factors. Indeed, the spectral betas are constant across scales.

Third, when $\sigma_{\varepsilon,u} < 0$ (and $\rho > 0$), the delayed adjustment model in Eq. (26) indicates that the excess asset return (y_t) is positively related to the lagged risk factor (x_{t-1}). Opposite to the intuition provided for Panel (a) of Figure 5, this implies that a positive shock to the risk factor at time $t-1$ had a positive effect on y_{t-1}, and also a positive effect on y at time t. However, it also holds that a negative shock at time $t-1$ in x has a negative effect on y at time $t-1$, and also a negative effect at time t (through x_{t-1}). Therefore, we expect systematic risk to increase with longer horizons, and thus also the spectral betas. In Panel (c) of Figure 5 we observe the spectral betas under $\sigma_{\varepsilon,u} = -0.3 < 0$. Consistent with our intuition and Eq. (26), the estimates of systematic risk increase with scale j.

Finally, we consider the situation in which $\rho = 0$ and $\sigma_{\varepsilon,u} = 0.3$. Following the delayed
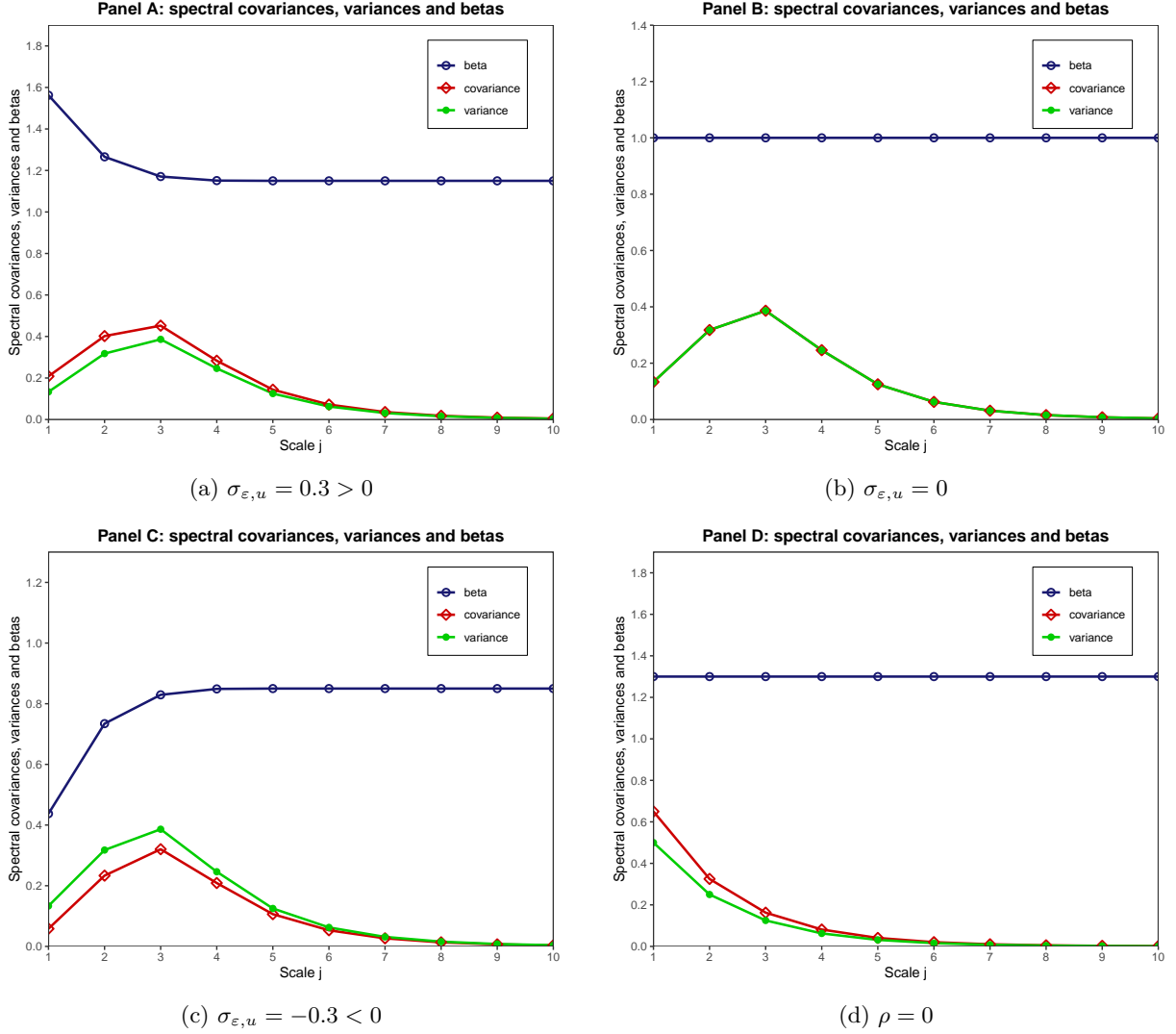
Figure 5: This figure shows the spectral covariance, spectral variances, and spectral betas obtained for different choices of $\sigma_{\varepsilon,u}$ (Eq. (26)). The models used for the excess asset return and risk factors are introduced in Appendix D.1. Panels (a), (b) and (c) we set $\rho = 0.5$, $\sigma_\varepsilon = 1$, and $\sigma_u = 1$. In Panel (d), we set $\rho = 0$ and $\sigma_\varepsilon = 0.3$.

adjustment model in Eq. (26), $\rho = 0$ should have the same effect as $\sigma_{\varepsilon,u} = 0$, because the excess asset returns are not related to lagged risk factors. Specifically, the delayed adjustment model in Eq. (26) can be formulated as $y_t = (\beta + \frac{\sigma_{\varepsilon,u}}{\sigma_\varepsilon^2})x_t + v_t$. This implies that if we estimate the traditional factor model in Eq. (22), we would obtain an inconsistent estimate of the overall beta (β). We observe the spectral betas in Panel (d) of Figure 5, which are constant across scales.

To conclude, we find that the dependence of the excess asset return on lagged risk factors (i.e., $\sigma_{\varepsilon,u} \neq 0$) implies frequency-specific spectral betas. Moreover, the lack of delayed adjustment (i.e., $\sigma_{\varepsilon,u} = 0$) leads to constant spectral betas over scales. However, the opposite pattern also holds: frequency-specific spectral betas imply the delayed adjustment of asset returns by risk factor, which we illustrate in the appendix below.

D.2 Frequency-specific betas imply delayed price adjustments

In this appendix, we follow the analysis of Bandi et al. (2021), and show that scale-varying spectral betas imply delayed price adjustments. First, we rewrite a spectral factor model with frequency-specific betas to a delayed adjustment model. Then, with a simulation study, we show that the correlation between the risk factors and the residuals of this delayed adjustment model depends on the spectral betas.

Let y_t and x_t be the excess asset return and risk factor at time t. We assume that both series are covariance stationary, and define a spectral factor model with $J = 1$ spectral components. Following Eq. (4), we get

$$y_t = \beta^{HF} x_t^{(1)} + \beta^{LF} x_t^{(>1)} + u_t \tag{35}$$

where $x_t^{(>1)} = x_t - x_t^{(1)}$, and u_t is an error term. Furthermore, β^{HF} and β^{LF} are the corresponding high-frequency (HF) and low-frequency (LF) spectral betas. The objective is to express the spectral factor model in Eq. (35) into a delayed adjustment model, where lagged risk factors (x_{t-1}) influence the excess asset return (y_t).

Under the assumption that the bivariate process $\mathbf{x} = \{(y_t, x_t)\}_{t \in \mathbb{Z}}$ is covariance stationary, we can use Eq. (13) to write this process in its Wold representation. This means that the risk factor, x_t, can be formulated as

$$x_t = \sum_{k=0}^{\infty} \begin{pmatrix} \alpha_k^3 & \alpha_k^4 \end{pmatrix} \begin{pmatrix} \varepsilon_{t-k}^1 \\ \varepsilon_{t-k}^2 \end{pmatrix} = \sum_{k=0}^{\infty} \boldsymbol{c}_k^{\mathsf{T}} \boldsymbol{\varepsilon}_{t-k}, \tag{36}$$

where $\boldsymbol{\varepsilon} = \{(\varepsilon_t^1, \varepsilon_t^2)\}_{t \in \mathbb{Z}}$ is a white noise process, and $\boldsymbol{c}_k = \begin{pmatrix} \alpha_k^3 & \alpha_k^4 \end{pmatrix}^{\mathsf{T}}$.

Now, using the Haar filter on the Wold residuals and coefficients, following Eq. (11) and Eq. (12), to derive

$$
\begin{aligned}
x_t^{(1)} &= \sum_{k=0}^{\infty} \left(\frac{\boldsymbol{c}_{2k} - \boldsymbol{c}_{2k+1}}{\sqrt{2}} \right)^{\mathsf{T}} \left(\frac{\boldsymbol{\varepsilon}_{t-2k} - \boldsymbol{\varepsilon}_{t-2k-1}}{\sqrt{2}} \right) \\
&= \left(\frac{\boldsymbol{c}_0 - \boldsymbol{c}_1}{\sqrt{2}} \right)^{\mathsf{T}} \left(\frac{\boldsymbol{\varepsilon}_t - \boldsymbol{\varepsilon}_{t-1}}{\sqrt{2}} \right) + \left(\frac{\boldsymbol{c}_2 - \boldsymbol{c}_3}{\sqrt{2}} \right)^{\mathsf{T}} \left(\frac{\boldsymbol{\varepsilon}_{t-2} - \boldsymbol{\varepsilon}_{t-3}}{\sqrt{2}} \right) + \cdots
\end{aligned} \tag{37}
$$

This means that the residual spectral component $x_t^{(>1)}$ can be written as

$$
\begin{aligned}
x_t^{(>1)} &= x_t - x_t^{(1)} \\
&= \left(\frac{\boldsymbol{c}_0 + \boldsymbol{c}_1}{\sqrt{2}} \right)^{\mathsf{T}} \left(\frac{\boldsymbol{\varepsilon}_t + \boldsymbol{\varepsilon}_{t-1}}{\sqrt{2}} \right) + \left(\frac{\boldsymbol{c}_2 + \boldsymbol{c}_3}{\sqrt{2}} \right)^{\mathsf{T}} \left(\frac{\boldsymbol{\varepsilon}_{t-2} + \boldsymbol{\varepsilon}_{t-3}}{\sqrt{2}} \right) + \cdots,
\end{aligned} \tag{38}
$$

where we used the fact that $x_t = x_t^{(1)} + x_t^{(>1)}$, as indicated by Eq. (13).

To observe that $x_t^{(>1)}$ can indeed be expressed as Eq. (38), we use the expression of $x_t^{(1)}$ in Eq. (37), to write

$$x_t = x_t^{(1)} + x_t^{(>1)} \tag{39}$$

$$= \left(\frac{\boldsymbol{c}_0 - \boldsymbol{c}_1}{\sqrt{2}}\right)^\intercal \left(\frac{\boldsymbol{\varepsilon}_t - \boldsymbol{\varepsilon}_{t-1}}{\sqrt{2}}\right) + \left(\frac{\boldsymbol{c}_0 + \boldsymbol{c}_1}{\sqrt{2}}\right)^\intercal \left(\frac{\boldsymbol{\varepsilon}_t + \boldsymbol{\varepsilon}_{t-1}}{\sqrt{2}}\right)$$

$$+ \left(\frac{\boldsymbol{c}_2 - \boldsymbol{c}_3}{\sqrt{2}}\right)^\intercal \left(\frac{\boldsymbol{\varepsilon}_{t-2} - \boldsymbol{\varepsilon}_{t-3}}{\sqrt{2}}\right) + \left(\frac{\boldsymbol{c}_2 + \boldsymbol{c}_3}{\sqrt{2}}\right)^\intercal \left(\frac{\boldsymbol{\varepsilon}_{t-2} + \boldsymbol{\varepsilon}_{t-3}}{\sqrt{2}}\right) + \cdots \tag{40}$$

where

$$\left(\frac{\boldsymbol{c}_{2k} - \boldsymbol{c}_{2k+1}}{\sqrt{2}}\right)^\intercal \left(\frac{\boldsymbol{\varepsilon}_{t-2k} - \boldsymbol{\varepsilon}_{t-2k-1}}{\sqrt{2}}\right) + \left(\frac{\boldsymbol{c}_{2k} + \boldsymbol{c}_{2k+1}}{\sqrt{2}}\right)^\intercal \left(\frac{\boldsymbol{\varepsilon}_{t-2k} + \boldsymbol{\varepsilon}_{t-2k-1}}{\sqrt{2}}\right)$$

$$= \frac{1}{2}\left(\boldsymbol{c}_{2k}^\intercal\left(\boldsymbol{\varepsilon}_{t-2k} - \boldsymbol{\varepsilon}_{t-2k-1}\right) - \boldsymbol{c}_{2k+1}^\intercal\left(\boldsymbol{\varepsilon}_{t-2k} - \boldsymbol{\varepsilon}_{t-2k-1}\right)\right)$$

$$+ \frac{1}{2}\left(\boldsymbol{c}_{2k}^\intercal\left(\boldsymbol{\varepsilon}_{t-2k} + \boldsymbol{\varepsilon}_{t-2k-1}\right) + \boldsymbol{c}_{2k+1}^\intercal\left(\boldsymbol{\varepsilon}_{t-2k} + \boldsymbol{\varepsilon}_{t-2k-1}\right)\right)$$

$$= \boldsymbol{c}_{2k}^\intercal\boldsymbol{\varepsilon}_{t-2k} + \boldsymbol{c}_{2k+1}^\intercal\boldsymbol{\varepsilon}_{t-2k-1}.$$

By taking that the sum over this expression from 0 to infinity, we obtain the expression as in Eq. (40). Obviously, the resulting expression of x_t is equal to the formulation in Eq. (36). To sum up, we have shown that the sum of expression of $x_t^{(>1)}$ in Eq. (38) and $x_t^{(1)}$ in Eq. (37) results in the formulation of x_t in Eq. (36). This means that we have verified the expression of $x_t^{(>1)}$ in Eq. (38).

Next, we continue our journey to write Eq. (35) as a delayed adjustment model. We follow Bandi et al. (2021), and rewrite $x_t^{(>1)}$ in Eq. (38) to

$$x_t^{(>1)} = \frac{x_{t-1}^{\text{odd}} + x_t^{\text{even}}}{2}, \tag{41}$$

where

$$x_{t-1}^{\text{odd}} = (\boldsymbol{c}_0 + \boldsymbol{c}_1)^\intercal\boldsymbol{\varepsilon}_{t-1} + (\boldsymbol{c}_2 + \boldsymbol{c}_3)^\intercal\boldsymbol{\varepsilon}_{t-3} + \cdots \tag{42}$$

$$x_t^{\text{even}} = (\boldsymbol{c}_0 + \boldsymbol{c}_1)^\intercal\boldsymbol{\varepsilon}_t + (\boldsymbol{c}_2 + \boldsymbol{c}_3)^\intercal\boldsymbol{\varepsilon}_{t-2} + \cdots \tag{43}$$

Then, we derive the delayed adjustment model from the spectral factor model in Eq. (35), where we first use the fact that $x_t^{(>1)}$ is $x_t - x_t^{(1)}$, giving

$$y_t = \beta^{HF} x_t^{(1)} + \beta^{LF} x_t^{(>1)} + u_t,$$

$$= \beta^{HF} x_t^{(1)} + \beta^{LF}(x_t - x_t^{(1)}) + u_t.$$

Next, we reformulate $x_t - x_t^{(1)}$, and use the expression of $x_t^{(>1)}$, to get

$$y_t = \beta^{LF} x_t + (\beta^{HF} - \beta^{LF}) x_t^{(1)} + u_t,$$

$$= \beta^{LF} x_t + (\beta^{HF} - \beta^{LF}) \left(x_t - \frac{x_{t-1}^{\text{odd}} + x_t^{\text{even}}}{2} \right) + u_t.$$

Finally, we can further simplify the equation above, and end up with the delayed adjustment model, given as

$$y_t = \beta^{HF} x_t + \left(\frac{\beta^{HF} - \beta^{LF}}{2} \right) (x_{t-1}^{\text{odd}} + x_t^{\text{even}}) + u_t, \tag{44}$$

$$= \beta^{HF} x_t + \widetilde{u}_t,$$

where $\widetilde{u}_t = \left(\frac{\beta^{HF} - \beta^{LF}}{2} \right) (x_{t-1}^{\text{odd}} + x_t^{\text{even}}) + u_t$.

We observe that Eq. (44) is a delayed adjustment model. Specifically, frequency-specific betas (i.e., $\beta^{HF} \neq \beta^{LF}$) imply the adjustment of excess asset return (y_t) by lagged risk factors (x_{t-1}^{odd}). However, when the spectral betas are constant across scales (i.e., $\beta^{HF} = \beta^{LF}$), Eq. (44) implies the lack of delayed price adjustment.   □

D.2.1   Simulation

In Appendix D.1, we showed that a non-zero correlation between the risk factor (x_t) and the residual (u_t) of the traditional factor model in Eq. (22) (i.e., $\sigma_{\varepsilon,u} \neq 0$), leads to frequency-specific betas. Now, we demonstrate that the reverse relationship also holds. Specifically, in the context outlined above, frequency-specific betas imply a correlation between the risk factor and residual $\widetilde{u}_t$ in Eq. (44). Furthermore, we show that the sign of this correlation depends on the difference between β^{HF} and β^{LF}, and is consistent with our discussion in Appendix D.1.

First, we provide a formal derivation of the sign of the covariance, and thus correlation, between x_t and $\widehat{u}_t$. We emphasise that the (white noise) residual term u_t of the spectral factor model in Eq. (35) is uncorrelated with $x_t^{(1)}$ and $x_t^{(>1)}$. Then, using the delayed adjustment model in Eq. (44), we get

$$\mathbb{C}(x_t, \widetilde{u}_t) = \mathbb{C} \left(x_t, \left(\frac{\beta^{LF} - \beta^{HF}}{2} \right) (x_{t-1}^{\text{odd}} + x_t^{\text{even}}) + u_t \right).$$

Then, substituting $x_t^{(>1)}$ by the expression given in Eq. (41), we get

$$\mathbb{C}(x_t, \widetilde{u}_t) = \mathbb{C} \left(x_t, \left(\beta^{LF} - \beta^{HF} \right) x_t^{(>1)} + u_t \right),$$

$$= \left(\beta^{LF} - \beta^{HF} \right) \mathbb{C} \left(x_t, x_t^{(>1)} \right) + \mathbb{C} \left(x_t, u_t \right),$$

$$= \left(\beta^{LF} - \beta^{HF} \right) \mathbb{C} \left(x_t, x_t - x_t^{(1)} \right) + \mathbb{C} \left(x_t^{(1)} + x_t^{(>1)}, u_t \right),$$

where we use the linear property of covariances to derive the second line above. Furthermore, we use the fact that $x_t = x_t^{(1)} + x_t^{(>1)}$ in the third expression. The last expression is rewritten to

$$\mathbb{C}(x_t, \widetilde{u}_t) = \left(\beta^{LF} - \beta^{HF}\right)\left[\mathbb{V}(x_t) - \mathbb{C}\left(x_t, x_t^{(1)}\right)\right] + \mathbb{C}\left(x_t^{(1)}, u_t\right) + \mathbb{C}\left(x_t^{(>1)}, u_t\right),$$
$$= \left(\beta^{LF} - \beta^{HF}\right)\left[\mathbb{V}(x_t) - \mathbb{C}\left(x_t, x_t^{(1)}\right)\right], \tag{45}$$

where we again use the covariance as a linear operator in the first expression above. Furthermore, in the second expression we use the exogeneity of u_t with the spectral components, $\mathbb{C}(x_t^{(1)}, u_t) = 0$ and $\mathbb{C}(x_t^{(>1)}, u_t) = 0$.

In this second step of the derivation, we find a closed-form expression for the variance and covariance in Eq. (45). However, in order to derive these terms, we need to impose a data generating process for the risk factor, x_t. We assume that x_t follows an AR(1) model: $x_t = \rho x_{t-1} + \varepsilon_t^2$, where $\rho < 1$, such that x_t is covariance stationary. Furthermore, ε_t^2 is a white noise process.

We start with the variance of the spectral factor.

$$\mathbb{V}(x_t) = \mathbb{V}(\rho x_{t-1} + \varepsilon_t^2),$$
$$= \rho^2 \mathbb{V}(x_{t-1}) + \mathbb{V}(\varepsilon_t^2),$$

where we use the white noise property of ε_t^2, and take the autoregressive coefficient outside the variance. Next, because x_t is covariance stationary, its variance is constant over time, this means that

$$(1 - \rho^2)\mathbb{V}(x_t) = \mathbb{V}(\varepsilon_t^2) = \sigma_\varepsilon^2,$$
$$\implies \mathbb{V}(x_t) = \frac{\sigma_\varepsilon^2}{1 - \rho^2}. \tag{46}$$

Now, we derive the covariance between the risk factor and its spectral component at scale $j = 1$, $\mathbb{C}(x_t, x_t^{(1)})$.

$$\mathbb{C}\left(x_t, x_t^{(1)}\right) = \mathbb{C}\left(x_t^{(1)} + x_t^{(>1)}, x_t^{(1)}\right),$$
$$= \mathbb{C}\left(x_t^{(1)}, x_t^{(1)}\right) = \mathbb{V}\left(x_t^{(1)}\right),$$

where we used the orthogonality between the spectral components, $x_t^{(1)}$ and $x_t^{(>1)}$. Using the expression for $x_t^{(1)}$ in Eq. (37), we rewrite the covariance above to

$$\mathbb{C}\left(x_t, x_t^{(1)}\right) = \mathbb{V}\left(\sum_{k=0}^{\infty}\left(\frac{\boldsymbol{c}_{2k} - \boldsymbol{c}_{2k+1}}{\sqrt{2}}\right)^{\mathsf{T}}\left(\frac{\boldsymbol{\varepsilon}_{t-2k} - \boldsymbol{\varepsilon}_{t-2k-1}}{\sqrt{2}}\right)\right).$$

Since x_t is an AR(1) process, a derivation similar as in Appendix D.1.1, tells us that $\boldsymbol{c}_{2k} = \rho^{2k}$,

---

Note that ε_t^2 is not the squared observation of a shock (ε) at time t. Instead, we use ε_t^2 to make the connection to the discussion in the previous section, see Eq. (36). We can show that $\boldsymbol{c}_k = \begin{pmatrix} 0 & \rho^k \end{pmatrix}^{\mathsf{T}}$.

and $\varepsilon_{t-k} = \varepsilon_{t-k}^2$ (i.e., the residual in the AR(1) for x_t). Therefore, we write the expression above as

$$
\begin{aligned}
\mathbb{C}\left(x_t, x_t^{(1)}\right) &= \mathbb{V}\left(\sum_{k=0}^{\infty}\left(\frac{\rho^{2k} - \rho^{2k+1}}{\sqrt{2}}\right)\left(\frac{\varepsilon_{t-2k}^2 - \varepsilon_{t-2k-1}^2}{\sqrt{2}}\right)\right), \\
&= \frac{1}{4}\sum_{k=0}^{\infty}\left(\rho^{2k} - \rho^{2k+1}\right)^2 \mathbb{V}\left(\varepsilon_{t-2k}^2 - \varepsilon_{t-2k-1}^2\right), \\
&= \frac{1}{4}(1-\rho)^2 \sum_{k=0}^{\infty}\left(\rho^{4k}\right)\left[\mathbb{V}\left(\varepsilon_{t-2k}^2\right) + \mathbb{V}\left(\varepsilon_{t-2k-1}^2\right)\right], \\
&= \frac{\sigma_\varepsilon^2(1-\rho)^2}{2(1-\rho^4)},
\end{aligned}
\tag{47}
$$

where we use the white noise properties of ε, and the closed-form expression for a geometric sum (note $|\rho| < 1$), in the last expressions above.

Finally, we use the variance of the risk factor in Eq. (46), and its covariance with the spectral component at scale $j = 1$ in Eq. (47), to derive a closed-form expression for the covariance between x_t and $\widetilde{u}_t$ in Eq. (45).

$$
\begin{aligned}
\mathbb{C}(x_t, \widetilde{u}_t) &= \left(\beta^{LF} - \beta^{HF}\right)\left[\mathbb{V}(x_t) - \mathbb{C}\left(x_t, x_t^{(1)}\right)\right], \\
&= \left(\beta^{LF} - \beta^{HF}\right)\left[\frac{\sigma_\varepsilon^2}{1-\rho^2} - \frac{\sigma_\varepsilon^2(1-\rho)^2}{2(1-\rho^4)}\right], \\
&= \left(\beta^{LF} - \beta^{HF}\right)\left(\frac{2\sigma_\varepsilon^2(1-\rho^4) - \sigma_\varepsilon^2(1-\rho)^2(1-\rho^2)}{2(1-\rho^2)(1-\rho^4)}\right), \\
&= \left(\beta^{LF} - \beta^{HF}\right)\left(\frac{\sigma_\varepsilon^2(1-\rho^2)\left[2(1+\rho^2) - (1-\rho)^2\right]}{2(1-\rho^2)(1-\rho^4)}\right), \\
&= \left(\beta^{LF} - \beta^{HF}\right)\left(\frac{\sigma_\varepsilon^2\left[1 + 2\rho + \rho^2\right]}{2(1-\rho^4)}\right), \\
&= \left(\beta^{LF} - \beta^{HF}\right)\underbrace{\left(\frac{\sigma_\varepsilon^2(1+\rho)^2}{2(1-\rho^4)}\right)}_{>0}.
\end{aligned}
\tag{48}
$$

In Eq. (48), we observe the final expression for $\mathbb{C}(x_t, \widetilde{u}_t)$. Since the variances in the denominator of the correlation are positive, the correlation between the risk factor and aggregate residual ($\widetilde{u}_t$) depends on the sign of $\beta^{LF} - \beta^{HF}$. If the low-frequency beta is larger than the high-frequency beta, then the correlation is positive. Similarly, when the high-frequency beta is larger than the low-frequency beta, the correlation is negative.

In order to illustrate the dependence of the correlation on the spectral betas, we conduct a simulation study, following Bandi et al. (2021). Specifically, we assume that the autoregressive coefficient of the AR(1) model is $\rho = 0.5$, $\sigma_\varepsilon^2 = 1$, and $\sigma_u^2 = 1$. Then, we generate ε_t and u_t from a independently and identically distributed normal distribution with mean zero, and a sample size of 10000 observations. These will be used in Eqs. (42) and (43) to get x_{t-1}^{odd} and x_t^{even},
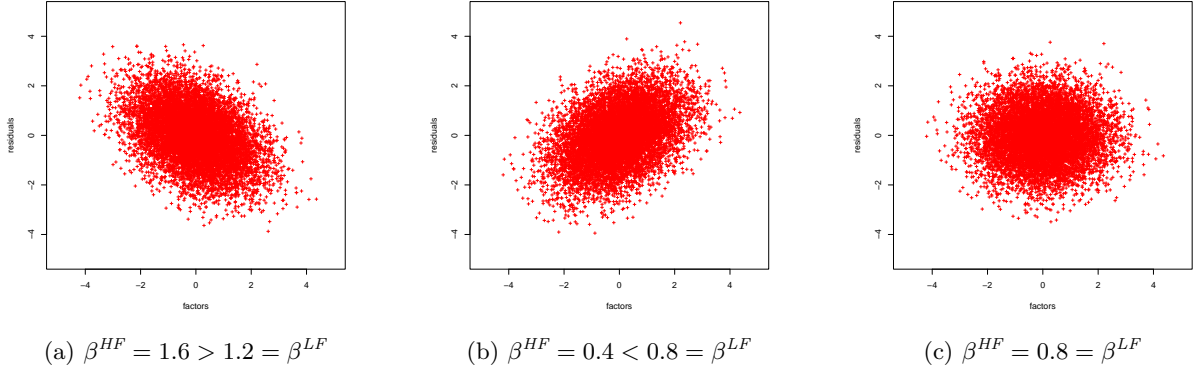
(a) $\beta^{HF} = 1.6 > 1.2 = \beta^{LF}$ (b) $\beta^{HF} = 0.4 < 0.8 = \beta^{LF}$ (c) $\beta^{HF} = 0.8 = \beta^{LF}$

Figure 6: Plot of risk factor, x_t, against the residual $\widetilde{u}_t$ in Eq. (44) for different choices of β^{HF} and β^{LF}. We generate 10000 observations with $\rho = 0.5$, $\sigma_\varepsilon^2 = 1$, and $\sigma_u^2 = 1$. The seed is set to 123.

respectively. Finally, we plot the simulated AR(1) process, x_t, against the shocks $\widetilde{u}_t$ (Eq. (44)), in Figure 6.

Note that $\widetilde{u}_t$ depends on the high- and low-frequency specific betas. Therefore, we consider two sets of values for the spectral betas. In Panel (a) of Figure 6 we use $\beta^{HF} = 1.6$ and $\beta^{LF} = 1.2$, such that $\beta^{HF} > \beta^{LF}$. We observe that the correlation between x_t and $\widetilde{u}_t$ is indeed negative, which is consistent with Eq. (48). Moreover, in Panel (b) of Figure 6 we plot the risk factors against the aggregated residuals with $\beta^{HF} = 0.4$ and $\beta^{LF} = 0.8$, such that $\beta^{HF} < \beta LF$. This panel shows that the correlation between x_t and $\widetilde{u}_t$ is positive, consistent with Eq. (48).

Finally, we extend the analysis by Bandi et al. (2021) with a new simulated environment. Specifically, we consider the situation in which $\beta^{HF} = 0.8 = \beta^{LF}$. Following the covariance derived in Eq. (44), we expect that x_t and $\widetilde{u}_t$ are uncorrelated. In other words, the delayed adjustment model in Eq. (44) will correspond to a traditional factor model with $\beta = \beta^{HF} = \beta^{LF}$, and y_t will not be influenced by the lagged risk factor x_{t-1}^{odd}. In Panel (c) of Figure 6, we observe that the risk factor and aggregate residual are indeed uncorrelated.

Also this is an interesting finding since, in Appendix D.1, we proved that delayed price adjustments (i.e., $\sigma_{\varepsilon,u} \neq 0$ in Eq. (26)) imply frequency-specific betas. Furthermore, the frequency-specific betas were constant across scales when $\sigma_{\varepsilon,u} = 0$ (i.e., no delayed price adjustment, see Panel (b) of Figure 5). We show in Panel (c) of Figure 6, that also the reverse relationship holds in our context: when $\beta^{HF} = \beta^{LF}$, then $\mathbb{C}(x_t, \widetilde{u}_t) = 0$.

Finally, this consistency between the discussion in Appendix D.1 and the discussion in this appendix, also holds for the other two panels in Figure 6. First, Panel (a) shows that when $\beta^{HF} > \beta^{LF}$, then the correlation between x_t and $\widetilde{u}_t$ is negative. In Appendix D.2 we discussed that β^{HF} is larger than β^{LF} when $\sigma_{\varepsilon,u} > 0$, as can be seen in Panel (a) of Figure 5. You might expect that this is inconsistent with Figure 6, however note that $\sigma_{\varepsilon,u}$ is not the correlation between x_t and a residual term including lagged effects of the risk factor. In Eq. (26), we observe that $\widetilde{v}_t = -\frac{\sigma_{\varepsilon,u}}{\sigma_\varepsilon^2}\rho x_{t-1} + v_t$ is this error with lagged effects that corresponds with $\widetilde{u}_t$ in this appendix. It can be shown that $\sigma_{\varepsilon,u} > 0$ implies a negative correlation between x_t and $\widetilde{v}_t$ in Eq. (26). This negative correlation between the risk factor and a residual (with lagged effects) is also what we observe in Panel (a) of Figure 6, which corresponds with $\beta^{HF} > \beta^{LF}$. Moreover, a similar connection with Appendix D.1 holds for Panel (b) of Figure 6.